

RESEARCH PAPER

# Oligogalacturonide application increases resistance to *Fusarium* head blight in durum wheat

Valentina Bigini<sup>1</sup>, Fabiano Sillo<sup>2</sup>, Sarah Giulietti<sup>1,3</sup>, Daniela Pontiggia<sup>3,4</sup>, Luca Giovannini<sup>2</sup>, Raffaella Balestrini<sup>2,\*</sup>, and Daniel V. Savatin<sup>1,\*</sup>

<sup>1</sup> Department of Agriculture and Forest Sciences, University of Tuscia, Via S. Camillo de Lellis, 01100 Viterbo, Italy

<sup>2</sup> National Research Council, Institute for Sustainable Plant Protection, Strada delle Cacce 73, 10135, Torino, Italy

<sup>3</sup> Department of Biology and biotechnologies 'Charles Darwin', Sapienza University of Rome, Ple Aldo Moro 5, 00185 Rome, Italy

<sup>4</sup> Research Center for Applied Sciences to the safeguard of Environment and Cultural Heritage (CIABC), Sapienza University of Rome, Ple Aldo Moro, 5 00185 Rome, Italy

\* Correspondence: [raffaellamaria.balestrini@cnr.it](mailto:raffaellamaria.balestrini@cnr.it) or [daniel.savatin@unitus.it](mailto:daniel.savatin@unitus.it)

Received 14 November 2023; Editorial decision 5 February 2024; Accepted 7 February 2024

Editor: Daolong Dou, Nanjing Agricultural University, China

## Abstract

**Fusariosis causes substantial yield losses in the wheat crop worldwide and compromises food safety because of the presence of toxins associated with the fungal disease. Among the current approaches to crop protection, the use of elicitors able to activate natural defense mechanisms in plants is a strategy gaining increasing attention. Several studies indicate that applications of plant cell-wall-derived elicitors, such as oligogalacturonides (OGs) derived from partial degradation of pectin, induce local and systemic resistance against plant pathogens. The aim of this study was to establish the efficacy of OGs in protecting durum wheat (*Triticum turgidum* subsp. *durum*), which is characterized by an extreme susceptibility to *Fusarium graminearum*. To evaluate the functionality of OGs, spikes and seedlings of cv. Svevo were inoculated with OGs, *F. graminearum* spores, and a co-treatment of both. Results demonstrated that OGs are active elicitors of wheat defenses, triggering typical immune marker genes and determining regulation of fungal genes. Moreover, bioassays on spikes and transcriptomic analyses on seedlings showed that OGs can regulate relevant physiological processes in Svevo with dose-dependent specificity. Thus, the OG sensing system plays an important role in fine tuning immune signaling pathways in durum wheat.**

**Keywords:** Cell wall, durum wheat, *Fusarium graminearum*, immune signaling, oligogalacturonides, transcriptomics.

## Introduction

Nowadays, worldwide crop losses from phytopathogens range from 17% to 30% for major agricultural crops, undermining the urgent goal of a 70% increase required to satisfy the food demand, and directly affecting food quality and human health (Savary *et al.*, 2019; Botticella *et al.*, 2021). *Fusarium* head blight (FHB), or fusariosis, is a destructive fungal disease

mainly caused by *Fusarium graminearum* (*Fg*) that can lead to a 50–70% loss of marketable grain (Alisaac and Mahlein, 2023). Besides reducing grain weight and quality during the infection, *Fusarium* species produce several trichothecene mycotoxins, including deoxynivalenol and nivalenol, which are toxic for humans and animals (Hägglom and Nordkvist, 2015),

representing a significant hazard in the food chain (Magan and Aldred, 2007). Additionally, climate changes are predicted to positively impact on the frequency and severity of FHB epidemics (Jung *et al.*, 2022).

Control strategies for fusariosis are still limited: in bread wheat, genetic variation for resistance to FHB is large and a multitude of resistance sources from 'foreign' and 'native' wheat germplasm are known (Steiner *et al.*, 2017). Conversely, durum wheat is notorious for its high susceptibility to FHB (Miedaner *et al.*, 2017), and breeding for FHB resistance is difficult due to the lack of resistance sources (Miedaner, 1997) as well as to difficulties in efficiently combining the numerous small-effect resistance quantitative trait loci (Steiner *et al.*, 2019). Therefore, new, harmless, and sustainable control strategies for FHB disease management are urgently required. The exploitation of the plant innate immunity is needed considering that, if activated timely, it can efficiently restrict plant infection by microorganisms (Bigini *et al.*, 2021). The innate immunity represents, in fact, the first step in defense against invaders and can be activated within a few minutes after sensing immunogenic signals derived both from pathogens and plant tissue damage (Abdul Malik *et al.*, 2020). The faster pathogen detection occurs, the sooner proper immune responses are mounted by plants, with a consequent higher probability to restrict or block the tissue invasion. An active route for fungus entry is penetration of the epidermal cuticle and cell wall with short infection hyphae (Mary Wanjiru *et al.*, 2002). As an enclosing barrier, the cell wall represents the first obstacle to fungal entry. *Fg* secretes a broad spectrum of cell wall-degrading enzymes used to overcome the plant cell wall and to facilitate the assimilation of nutrients (Henrissat, 1991; Yang *et al.*, 2012; Kubicek *et al.*, 2014; Benedetti *et al.*, 2019).

Pectin degradation by fungal polygalacturonases favors the accumulation of oligomeric homogalacturonan degradation intermediates, i.e. oligogalacturonides (OGs), recognized as danger signals by plant specific receptors and able to activate downstream immune responses (Ferrari *et al.*, 2013; Savatin *et al.*, 2014; De Lorenzo and Cervone, 2022). More than 40 years ago, phytoalexin accumulation in soybean cotyledons provided the first evidence that pectin fragments activate defensive responses (Hahn *et al.*, 1981). These fragments were later identified as oligomers of  $\alpha$ -1,4-linked galacturonosyl residues (Nothnagel *et al.*, 1983). OGs are nowadays probably the best characterized plant damage associated molecular patterns (DAMPs) and can elicit a wide range of defense responses in several plant species (Desaki *et al.*, 2012; Ferrari *et al.*, 2013; Pontiggia *et al.*, 2020). An important aspect to be considered is that different degrees of polymerization (DP) of OGs determines their physiological properties and biological function. Different studies have demonstrated that long OGs (DP>10) are the most effective in modulating immune signaling, while short OGs have little or no effect in Arabidopsis (Ferrari *et al.*, 2007; Denoux *et al.*, 2008). However, other studies have suggested that also short OGs (DP<10) can impact plant defense

(Simpson *et al.*, 1998) and development (Miranda *et al.*, 2007; Pontiggia *et al.*, 2020). For instance, short OGs (DP4–6, DP2, and DP1–7) were shown to induce immune marker genes in potato and tomato and the synthesis of phytohormones in tobacco and tomato (Simpson *et al.*, 1998; Norman *et al.*, 1999; Montesano *et al.*, 2001). Furthermore, Davidsson *et al.* (2017) investigated the role of trimers (DP3). Transcriptomic analysis of Arabidopsis exposed to such compounds suggested that DP3 may induce the expression of genes involved in the plant defense, even if gene expression induced by trimers was generally not as strong as that induced by long OGs. However, a few studies were made to examine the effects of OGs in wheat plants (Randoux *et al.*, 2010; Ochoa-Meza *et al.*, 2021), though none described their role in resistance to fusariosis.

Over the years, one contentious issue has been whether *Fg* exhibits a biotrophic lifestyle during the initial stages of infection of floral tissues (Trail, 2009; Brown *et al.*, 2010; Erayman *et al.*, 2015; Chen *et al.*, 2021). A detailed microscopic study of the *Fg* infection process in wheat heads found no indication of necrotrophy at the initial stages of infection, as the advancing *Fg* hyphae remained in the intercellular spaces of wheat rachis cells before subsequent intracellular growth, which presumably leads to subsequent cell death and necrosis (Brown *et al.*, 2010). Therefore, *Fg* may be classified as a hemibiotrophic pathogen. Ding *et al.* (2011) demonstrated that resistance to *Fg* infection is associated with coordinated and ordered expression of diverse defense signaling pathways and altered secondary metabolism. Furthermore, Zhang *et al.* (2012) observed that the genes associated with the fungus non-symptomatic stage are involved in primary metabolic pathways, whereas transcripts corresponding to genes involved in cell wall degradation dominate the later growth stage of the infection process. Notably, the comparison of the transcriptomes of *Fg* feeding on living or dead tissues suggests that the fungus uses host signals to modulate the expression of several genes (Boedi *et al.*, 2016). Some fungal genes are repressed by host signals (Boedi *et al.*, 2016). On the other hand, host signal sensing is also required for the activation of deoxynivalenol biosynthesis. Deoxynivalenol is a virulence factor in wheat, causing tissue necrosis and allowing the fungus to spread into the rachis from florets in wheat (Jansen *et al.*, 2005; Bian *et al.*, 2021).

Numerous studies indicate that local application of cell wall-derived elicitors, such as OGs, induces broad-spectrum, long-lasting, and systemic resistance against pathogens in different plant species, such as Arabidopsis, rice, grapevine, and tomato (Aziz *et al.*, 2006; Moscatiello *et al.*, 2006; Ferrari *et al.*, 2007; Gamir *et al.*, 2021). The aim of this study was to investigate the role of OGs in the durum wheat–*Fg* interaction. Data here reported clearly show that OGs are perceived as danger signals capable of inducing immune responses and resistance to fusariosis in durum wheat cotyledons and spikes. To facilitate the elucidation of molecular mechanisms regulating plant defense activation upon OG sensing, RNA sequencing was carried out to obtain a general view of the transcriptome in

durum wheat seedlings inoculated with OGs at different concentrations (10 and 500  $\mu\text{g ml}^{-1}$ ), *Fg* spores, or a co-treatment of both OGs and fungus spores. Chitosan (CHIT, 100  $\mu\text{g ml}^{-1}$ ) was used as a positive control in the experimental set-up. The knowledge on the OG biology in durum wheat here generated will allow us to shed light on the role of DAMP signaling in cereals and open new perspectives on the application of molecular engineering approaches to strengthen plant immune responses against *Fg* and, possibly, other pathogenic microorganisms.

## Materials and methods

### Plant and fungal growth conditions

Plant material was prepared according to the protocol described in Jia *et al.* (2017). Wheat (*Triticum turgidum* subsp. *durum*) seeds cv. Svevo were rinsed with running water and then soaked overnight at 4 °C in a 500 ml flask containing sterile water to help seeds to break dormancy and germinate faster. The imbibed seeds were placed in Petri dishes (90 mm diameter) containing two layers of sterile paper and germinated in the dark for 2 d at 25 °C in a growth chamber. Germinated seeds were then transplanted to 24-well cell culture plates, one seed per well, and grown in the growth chamber for 1 d under controlled environment conditions at 25 °C with a 16 h light (450–500  $\mu\text{mol m}^{-2} \text{s}^{-1}$ ) and 8 h dark photoperiod.

The fungal pathogen *Fg* strain 3827 was cultured at 25 °C on potato dextrose agar (PDA) medium (AppliChem GmbH; Darmstadt, Germany). To induce macroconidia production, the fungus was cultured at 25 °C on synthetic nutrient agar (SNA) medium (Urban *et al.*, 2002) containing 0.1%  $\text{KH}_2\text{PO}_4$ , 0.1%  $\text{KNO}_3$ , 0.1%  $\text{MgSO}_4 \cdot 7\text{H}_2\text{O}$ , 0.05% KCl, 0.02% glucose, 0.02% sucrose, 2% bactoagar (Becton Dickinson; Franklin Lakes, NJ, USA). Macroconidia were harvested from 90 mm SNA agar plates after 10 d of incubation by adding 1 ml sterile water and scraping off conidiospores with a spatula. Conidia concentration was estimated with a Thoma chamber, adjusting the concentration to the proper concentration for the infection assays. For long-term storage at –80 °C, conidiospore suspensions were prepared to a density of  $10^6$  spores  $\text{ml}^{-1}$  in 10% glycerol.

In order to investigate the direct effect of OGs on *Fg* spore germination and mycelium growth, *Fg* spores ( $10^4$  conidia) were placed in PDA plates containing different amounts (10 or 500  $\mu\text{g ml}^{-1}$ ) of OGs. CHIT (2, 20, or 100  $\mu\text{g ml}^{-1}$ ) was used as positive control. A mock control was also included. The plates were incubated in the dark for 5 d at 24 °C. The mycelial growth was evaluated by measuring four fungal colony diameters from each plate by using the freely available ImageJ software (<http://rsbweb.nih.gov/ij/>). Data were obtained from three independent experiments, each one consisting of five replicates for each elicitor and concentration tested.

Oligogalacturonides were prepared according to the protocol described in Pontiggia *et al.* (2015). High molecular mass unmethylated polygalacturonic acid (PGA; Alfa Aesar) was solubilized in 100 ml of sodium acetate 50 mM, pH 5.0 to a concentration of 2% (w/v). The solution was digested for 180 min with 0.018 reducing group unit of *Aspergillus niger* endoPG, and the enzyme was inactivated by boiling the digest at 100 °C for 10 min in a water bath. After enzyme inactivation, the sample was diluted with 50 mM sodium acetate to a concentration of 0.5% PGA. To precipitate OGs, ethanol was added to the digest to a final concentration of 17% (v/v); the sample was incubated overnight at 4 °C with shaking and then centrifuged for 30 min at 30 000 *g*. OGs, recovered in the pellet, were re-dissolved in water, dialysed against water in a dialysis tube with a molecular mass cut-off of 1000 Da (Spectra/Por), and lyophilized. OGs were analysed by high-performance anion exchange with pulsed amperometric detection (HPAEC-PAD) with an ICS-6000

apparatus (Thermo Fisher Scientific, Waltham, MA, USA) equipped with a CarboPac PA100 3 × 250 mm analytical column with a guard column (Thermo Fisher Scientific). A flow of 0.4  $\text{ml min}^{-1}$  was used, and the temperature was kept at 35 °C. The injected samples (10  $\mu\text{g}$ ) were separated using a gradient with 0.05 M NaOH (A) and 1 M Na-acetate in 0.05 M NaOH (B): 0–30 min from 20% B to 90% B, 30–32 min at 90% B. Before injection of each sample, the column was equilibrated with 80% A and 20% B for 10 min. For matrix-assisted laser desorption/ionization (MALDI) MS analysis, the matrix solution was prepared by dissolving 2,5-dihydroxybenzoic acid in a solution of 70% acetonitrile with 0.1% trifluoroacetic acid to a final concentration of 20  $\text{mg ml}^{-1}$ . The samples (5  $\text{mg ml}^{-1}$  in water) were pre-treated for 10 min with Bio-Rex MSZ501 cation exchange resin beads (Bio-Rad Laboratories, Hercules, CA, USA) and then prepared as dried-droplets by spotting 1  $\mu\text{l}$  of matrix solution first on the stainless steel MALDI target and adding 1  $\mu\text{l}$  of sample solution immediately afterward. MALDI–time of flight (TOF)–MS measurements were performed on an UltrafleXtreme TOF/TOF mass spectrometer equipped with a reflector and controlled by the FlexControl 2.2 software package (Bruker Daltonics).

Shrimp shell chitosan (molecular mass 190–375 kDa, degree of deacetylation  $\geq 75\%$ , CAS number 9012-76-4, cat. no. 417963) was purchased from Merck (Darmstadt, Germany). Chitosan stock solution (10  $\text{mg ml}^{-1}$ ) was prepared by dissolving the required amount of chitosan powder in 1 M acetic acid. The stock solution was autoclaved and subsequently added to sterile distilled water to obtain desired final chitosan concentrations.

### Fusarium graminearum infection assay in wheat spikes and seedlings

Wheat seeds cv. Svevo were surface sterilized with 75% (v/v) ethanol for 2 min, 40% (v/v) sodium hypochlorite for 15 min and then rinsed thoroughly in sterile water. Seed germination was performed in Petri dishes (90 mm diameter) containing two layers of sterile paper. When seminal roots and the hypocotyls emerged, around 10 d post-germination, seedlings were transferred in jiffy pots with soil, and vernalized at 4 °C for 1 month. Afterwards, plants were grown in a climatic chamber at 18–23 °C with a 16 h light (450–500  $\mu\text{mol m}^{-2} \text{s}^{-1}$ ) and 8 h dark photoperiod. When plants presented the second/third leaf, they were two by two transferred to 14 × 14 cm pots. PDA medium (AppliChem GmbH; Darmstadt, Germany) was used for the growth and maintenance of *Fg* strain 3827, and SNA medium was used to promote sporulation, as described previously.

Inoculation assays on wheat spikes cv. Svevo were conducted as reported by Makandar *et al.* (2012). At anthesis stage, inoculation of wheat plants was performed by single-spikelet inoculation. Briefly, the glumes of two opposite central florets of a wheat head were inoculated with OGs (500  $\mu\text{g ml}^{-1}$ ), *Fg* spores ( $2 \times 10^4$  conidia), and a co-treatment of both OGs and fungus spores. Sterile water was used as mock treatment and CHIT (100  $\mu\text{g ml}^{-1}$ ) as a positive control in the experimental set-up. High humidity conditions were maintained for 3 d by covering the inoculated spikes with a plastic bag. Over time, the fungal infection spread out to the other spikelets within each spike. FHB disease symptoms were assessed by counting the number of visually diseased spikelets at different days post-infection (dpi) and by relating them to the total number of spikelets of the respective head, resulting in a percentage of symptomatic spikelets. The final count was taken at 21 dpi. For each experiment, at least 15 plants per treatment were used.

To investigate the capability of OGs to induce immune responses and resistance systemically, we germinated and grew wheat seedlings on half MS containing 10, 100, or 500  $\mu\text{g ml}^{-1}$  OGs and 2, 20, or 100  $\mu\text{g ml}^{-1}$  CHIT for 3 d before inoculating *Fusarium* spores in coleoptiles as reported by Jia *et al.* (2017). Briefly, the top 1–2 mm of 3-day-old wheat coleoptiles were cut off and inoculated with *Fg* spores ( $2 \times 10^3$  conidia). Sterile water was used as mock treatment. The inoculated seedlings were

grown in a climatic chamber for 7 d under controlled environment conditions at 24 °C with a 16 h light (450–500  $\mu\text{mol m}^{-2} \text{s}^{-1}$ ) and 8 h dark photoperiod and 95% relative humidity. Lesion size on coleoptiles of inoculated wheat seedlings was measured at different dpi. The final measurement was taken at 7 dpi. The longitudinal length of brown lesions on wheat coleoptiles was measured as the lesion size at the indicated time by using ImageJ software. For each experiment, at least 15 seedlings per treatment were used.

#### Quantification of fungal biomass in durum wheat seedlings and spikes

Genomic DNA from different inoculated seedlings and spikes was extracted with Nucleospin Plant II kit (Macherey–Nagel, Oensingen, Switzerland) according to manufacturer's instructions. After a quality and quantity check, a quantitative real-time polymerase chain reaction (qPCR) was performed by using a CFX96 Real-Time System (Bio-Rad Laboratories) and amplifying 50 ng of gDNA in a 20  $\mu\text{l}$  reaction mixture containing 1 $\times$  SsoAdvanced Universal SYBR green Supermix (Bio-Rad Laboratories) and 0.5  $\mu\text{M}$  of each primer. qPCR data analysis was performed by using LinRegPCR software. The DNA content of the *Fg*  $\beta$ -tubulin gene (*Fg*  $\beta$ -*tubulin*), relative to the wheat actin gene (*TdACTIN*), was determined in wheat seedlings (7 dpi) and spikes (6, 24, and 48 hours post infection (hpi)) inoculated with *Fg* spores and with co-treatment of both OGs and fungus spores. Results were determined by using the Pfaffl method (Pfaffl, 2001) and expressed in arbitrary units. Primer sequences are shown in Supplementary Table S1.

#### Elicitor treatments in durum wheat seedlings

Following sterilization (see above) seeds were washed three times with sterile water and placed in Petri dishes (90 mm diameter) containing sterile paper. Three days after germination, seedlings were transferred in sterile culture tubes containing half-strength MS medium supplemented with sucrose 0.5% (w/v) (Sigma–Aldrich) and solidified with agar 0.8% (w/v) (Duchefa Biochemie; Haarlem, The Netherlands) at pH 5.8, in the absence or presence of different concentrations (10 or 500  $\mu\text{g ml}^{-1}$ ) of purified OGs. Chitosan (2, 20, or 100  $\mu\text{g ml}^{-1}$ ) was used as a known compound affecting wheat growth in the experimental set-up (Liu *et al.*, 2021). After 7 d in a growth chamber at 24 °C with a 16 h light (450–500  $\mu\text{mol m}^{-2} \text{s}^{-1}$ ) and 8 h dark photoperiod, fresh weight, root length, and first leaf length were measured for each seedling. The root length and the first leaf length of all plantlets were measured by using the freely available ImageJ software.

#### RNA sequencing

Three-day-old wheat seedlings were inoculated with OGs (10 and 500  $\mu\text{g ml}^{-1}$ ), *Fg* spores ( $2 \times 10^5$  conidia), and a co-treatment of both OGs and fungus spores. Sterile water was used as mock treatment (control), and CHIT (100  $\mu\text{g ml}^{-1}$ ), whose priming ability has already been demonstrated (Deshaies *et al.*, 2022), was also included in the experimental set-up. Three biological replicates for each condition were selected at 48 hpi: mock; plants elicited with chitosan (100  $\mu\text{g ml}^{-1}$  (CHIT100)); plants elicited with OGs (10  $\mu\text{g ml}^{-1}$  (OG10) and 500  $\mu\text{g ml}^{-1}$  (OG500)); plants inoculated with *Fg*; and plants inoculated with *Fg* and co-treated with elicitor compounds (*Fg*+CHIT100, *Fg*+OG10, *Fg*+OG500). For each sample, fresh plant material (approximately 100 mg) was frozen with liquid nitrogen, ground in 2 ml tubes by using steel beads (diameter 0.4 mm) and homogenized through a TissueLyser II (Qiagen, Valencia, CA, USA). Total RNA was isolated by using a cetyltrimethylammonium bromide-based lysis buffer following the 'pine tree method' (Chang *et al.*, 1993). The RNA pellet was resuspended in diethylpyrocarbonate-treated water and quality of the extracted RNA was determined by using a Nanodrop

2000 spectrophotometer (Thermo Fisher Scientific). Library preparation and RNA sequencing were performed by Genartis s.r.l. laboratories (Verona, Italy). In total, 24 Illumina RNA-seq libraries were generated using the TruSeq stranded mRNA ligation kit (Illumina) from 700 ng of RNA samples, after poly(A) capture and according to manufacturer's instructions. Using the Agilent 4150 Tape station (Agilent Technologies), capillary electrophoretic analysis was carried out to measure the quality and size of the RNAseq libraries. Libraries were quantified by real-time PCR against a standard curve with the KAPA Library Quantification Kit (Kapa Biosystems, Wilmington, MA, USA) and sequenced with Illumina technology in 150PE mode on a Novaseq6000 sequencer. Raw reads from RNA-seq were submitted to NCBI Sequence Read Archive (Bioproject PRJNA977839).

#### RNA-seq data analysis and differential gene expression quantification

The RNA-sequencing-obtained reads were aligned to the transcriptome of durum wheat (Maccaferri *et al.*, 2019) available at <https://plants.ensembl.org/> using the Salmon software v1.4.0 (Patro *et al.*, 2017). Salmon uses a quasi-mapping approach to align the reads, which allows for more sensitive and accurate alignment compared with traditional methods. This software estimates the relative abundance of different transcripts as transcripts per million (TPM), a normalization method computed considering the library size, number of reads, and the effective length of the transcript (Patro *et al.*, 2017). Raw read counts and TPM data were generated from each Salmon output file, by combining isoform counts to obtain counts at gene level. The outputs including transcript lengths, count of aligned reads, and abundance estimates were imported in DESeq2 by using the R package tximport v1.22.0 (Soneson *et al.*, 2015) using the length ScaledTPM method. Principal component analysis was performed on normalized gene counts (regularized log transformation of normalized data) using the DESeq2 package v1.34.0 (Love *et al.*, 2014). The data were used to identify differentially expressed genes (DEGs) using the DESeq2 package v1.34.0 (Love *et al.*, 2014). The variance on reads count was calculated based on the three biological replicates per condition by applying a negative binomial distribution to model the count data and identify genes with significant changes in expression between the different conditions. The DEG identification was performed after normalization of the count data and correction for multiple testing, both accounted by DESeq2, through a Wald test, and using the mock condition (water treatment) as control. Variance on reads count was calculated based on the three biological replicates per condition. During DESeq2 analysis, shrinkage estimation of effect size (log fold change (LFC) estimates) was used, in order to generate more accurate  $\log_2$  fold change ( $\log_2\text{FC}$ ) estimates and taking into account variability among replicates. A threshold of adjusted  $P < 0.05$  was used to identify DEGs. A cut-off of the  $P$ -adjusted value  $\leq 0.05$  was used to classify a gene as differentially expressed in comparison with the control. Both the identified DEGs and all transcripts of the Svevo transcriptome were annotated through Blast2GO v5.2.5 (Conesa *et al.*, 2005) to obtain an updated functional annotation and to assign their associated Gene Ontology (GO) terms. The identified DEGs were then analysed for functional enrichment using Blast2GO to reveal the biological processes, pathways, or other functional categories that are enriched among the DEGs. To perform GO enrichment analysis and to provide a summary of the functions and pathways associated to the obtained sets of DEGs, the ShinyGO v0.77 online tool was used (Ge *et al.*, 2020). In addition, reads obtained from samples inoculated with *Fg*, as well as from samples inoculated and co-treated with both OGs and CHIT100, showing no alignment on plant transcriptome, were aligned using Salmon on *F. graminearum* transcriptome strain PH-1 (Cuomo *et al.*, 2007) available at the MycoCosm web portal of the Joint Genome Institute (JGI; <https://mycocosm.jgi.doe.gov/Fusgr1/Fusgr1.home.html>). The same pipeline used for plants via tximport v1.22.0 was

used for detecting reads putatively belonging to the fungus. By using *Fg*-inoculated samples without OGs as reference, DESeq2 v1.34.0 was used to assess fungal DEGs (threshold of adjusted  $P < 0.05$ ).

#### Validation of RNA-seq through RT-qPCR on selected genes

The differential expression of 11 selected DEGs obtained from RNA-seq analysis was validated through RT-qPCR. The RNA samples from the three biological replicates for each condition assessed through RNA-seq (for a total of 24 samples) were treated with TURBO DNA-free Kit (Thermo Fisher Scientific) to remove genomic DNA, whose absence was verified by PCR using primers designed on the reference gene coding for glyceraldehyde 3-phosphate dehydrogenase (GAPDH) (GenBank accession: EU022331.1). The RNA was then converted into cDNA by using the SuperScript II Reverse Transcriptase kit (Thermo Fisher Scientific), starting from 1  $\mu\text{g}$  of RNA per sample. The RT-qPCR reactions were performed in the Connect Real-Time PCR Detection System (Bio-Rad Laboratories), using the Power SYBR Green PCR Master Mix (Bio-Rad Laboratories). The primers used for the amplification (Supplementary Table S1) were designed on the coding sequences of the selected genes using the online software Primer3 (<https://primer3.ut.ee/>). The obtained cDNA was diluted 1:3 to be used as a template for the reactions, and two technical replicates were used for each of the three biological ones. Each RT-qPCR reaction was performed on a total volume of 10  $\mu\text{l}$ , containing 1  $\mu\text{l}$  cDNA, 15  $\mu\text{l}$  Power SYBR Green PCR Master Mix (Bio-Rad Laboratories) and 0.2  $\mu\text{l}$  of each primer (final concentration of 200 nM), using a 96-well plate. The following PCR protocol, which includes the calculation of the melting curve, was used: 95  $^{\circ}\text{C}$  for 30 s, 40 cycles of 95  $^{\circ}\text{C}$  for 10 s and 60  $^{\circ}\text{C}$  for 30 s, ramp from 65  $^{\circ}\text{C}$  to 95  $^{\circ}\text{C}$  with a temperature increment of 0.5  $^{\circ}\text{C}$  and a read plate every 5 s. For the normalization of gene expression data, two reference genes, i.e. one coding for GAPDH and one for actin (GenBank accession: AB181991.1), were used. The  $\Delta\Delta C_t$ , where  $\Delta\Delta C_t$  represents the  $\Delta C_{t,\text{sample}} - \Delta C_{t,\text{control}}$  (mock), was used to calculate the fold change for each tested gene (Livak and Schmittgen, 2001) and the results obtained by RT-qPCR and RNA-seq were compared using Pearson's correlation coefficient.

#### Statistical analysis

Data were analysed with Student's *t*-test or ANOVA by using the SYSTAT 12 software (Systat Software Inc., San Jose, CA, USA). When significant *F*-values were observed ( $P < 0.05$ ), a pairwise analysis was carried out by the Tukey honestly significant difference test (Tukey test).

## Results

### *Oligogalacturonides trigger resistance to F. graminearum in durum wheat spikes*

To evaluate the functionality of OGs as elicitors of immunity and their ability to restrict phytopathogen fungal growth in durum wheat spikes at the anthesis stage, two opposite central florets of a wheat head were inoculated with OGs (500  $\mu\text{g ml}^{-1}$ ), *Fg* spores ( $2 \times 10^4$  conidia), and a co-treatment of both OGs and fungus spores. Before the treatment, degree of polymerization of the corresponding oligomers was characterized by HPAEC-PAD and MALDI-TOF analyses (Supplementary Fig. S1). Sterile water was used as mock treatment and CHIT (100  $\mu\text{g ml}^{-1}$ ) as a positive control in the experimental set-up. We observed that symptom progression was slower in spikes co-treated with OGs and fungus spores

than in spikes inoculated with the fungus alone. The maximal reduction of 25% in symptom severity was detected between 7 and 13 dpi (Fig. 1A). At this infection stage, several OG-co-treated inoculated spikelets showed a temporary block of the infection. The spikes co-treated with CHIT and *Fg* did not show symptoms of the fungal disease (Fig. 1A), likely because of the inhibitory effect of CHIT on *Fg* spore germination and hyphal development (Deshaies *et al.*, 2022). The fungal abundance in the different treatments was monitored by quantifying the DNA accumulation through qPCR and amplifying the *Fg*  $\beta$ -tubulin gene, and was significantly lower in spikes of plants co-treated with fungus and elicitors. With the OG co-treatment, the fungal DNA amount was 84.6%, 61.5%, and 84.4% compared with spikes inoculated with the fungus alone at 6, 24, and 48 hpi, respectively (Fig. 1B). Interestingly, results showed that, compared with the *Fg* control condition, in the CHIT and *Fg* co-treatments the fungal amount was only 4.6%. As shown in Fig. 1C, at 10 dpi the severity of the symptoms was particularly evident in plants inoculated with the fungus alone, displaying 100% of the spikelets infected. On the contrary, spikes co-treated with OGs showed a considerably lower severity of the disease at this time point of the infection.

### *Impact of oligogalacturonides on wheat agronomical and growth parameters*

After verifying that OGs and CHIT can limit the infection spread of *Fg*, we evaluated the impact of the elicitors on important wheat agronomical and growth parameters after infection. The number of seeds per spike, the number of seeds per spikelet, the primary spike weight, the weight of seeds per spike, the weight of 1000 seeds, and the yield loss were analysed (Fig. 2). In the *Fg*-inoculated plants, significantly lower yield values were observed for all the parameters considered. The number of seeds per spike and per spikelet were inhibited by 77.6% and 76.9%, respectively, compared with untreated plants (Fig. 2A, B). Moreover, results showed an inhibition of the primary spike weight, the weight of seeds per spike and the weight of 1000 seeds by 77.3%, 95.1%, and 73.8%, respectively (Fig. 2C–E). Interestingly, no significant differences were observed compared with mock condition in plants co-treated with CHIT and the fungus.

In the presence of OG co-treatments, higher yield values were observed compared with *Fg*-inoculated plants. The inhibition percentages of the number of seeds per spike and per spikelet were 35.3% and 29.2%, respectively, compared with untreated plants (Fig. 2A, B). For the primary spike weight, the weight of seeds per spike, and the weight of 1000 seeds, a significant reduction of 36.6%, 38.9%, and 48.6%, respectively, was observed (Fig. 2C–E). Therefore, OGs limit the infection spread of *Fg* as well as the yield loss associated to fungal disease. The loss in production was then calculated and expressed as a percentage (Fig. 2F). *Fg*-inoculated plants displayed a production loss of 79.7%, while OG-co-treated plants exhibited

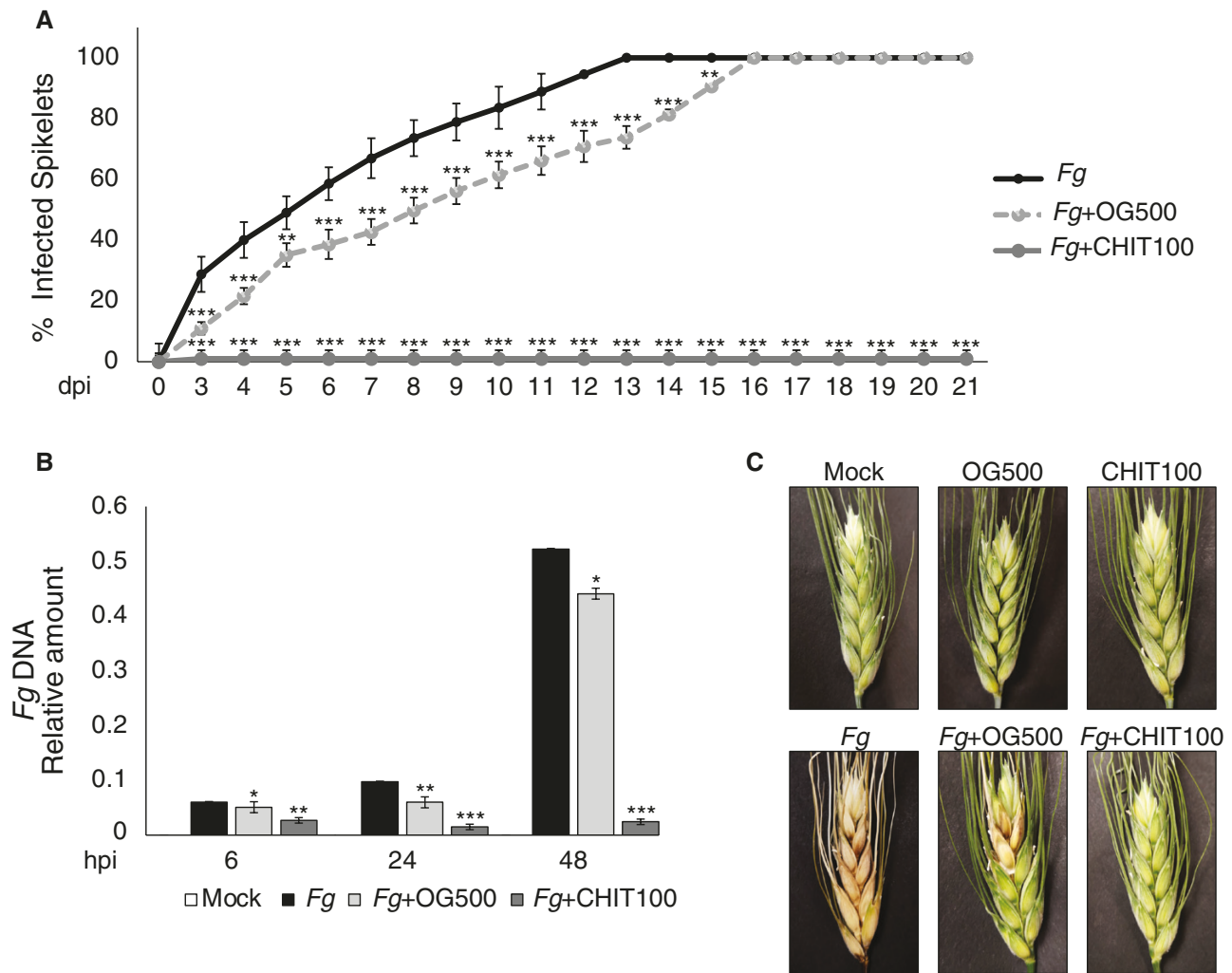


**Fig. 1.** Oligogalacturonides (OGs) trigger resistance to *Fusarium* head blight in cv. Svevo spikes. (A) Disease severity in the cultivar Svevo inoculated with *Fg*, *Fg*+OG, or *Fg*+CHIT co-treatment. Disease progression was monitored for 21 dpi. (B) *Fg* DNA quantification by real-time PCR analysis of  $\beta$ -*tubulin* gene normalized to the *TdACTIN* gene in spikes at 6, 24, and 48 hpi. (C) Images showing disease spread in representative wheat spikes for each treatment condition. Images were taken at 10 dpi. All values are means  $\pm$ SE ( $n=15$ ). Asterisks above the bars indicate values that are significantly different from seedlings inoculated with the *Fg* alone (\* $P<0.05$ , \*\* $P<0.01$ , \*\*\* $P<0.001$ , Student's *t*-test).

a yield reduction of only 28.3% compared with the mock condition. No significant differences were observed between CHIT-co-treated and untreated plants.

The quality and the filling of kernels were also evaluated, considering the length and the width of wheat seeds, after *Fg* infection. As shown in Fig. 3A, B, OG and CHIT treatments did not affect wheat seed length and width. On the contrary, the fungus *Fg* negatively impacted on both considered parameters by compromising the good filling of kernels and causing their shriveling.

Seeds derived from *Fg*-inoculated spikes displayed an inhibition of seed length and width of 33.4% and 43.75%, respectively, compared with the untreated condition. No significant differences in seeds derived from CHIT-co-treated plants were observed compared with mock condition. Moreover, we

observed that in the presence of OG-co-treatment, seeds displayed a reduced shriveling (Fig. 3C) and an inhibition of length and width of only 6.5% and 25%, respectively (Fig. 3A, B).

#### *Oligogalacturonides trigger resistance to F. graminearum in durum wheat seedlings*

The OG-related effects on plant morphological parameters were assessed by growing durum wheat seedlings, cv. Svevo, on MS medium in the absence or presence of different concentrations (10 or 500  $\mu\text{g ml}^{-1}$ ) of purified OGs for 7 d. CHIT (2, 20, or 100  $\mu\text{g ml}^{-1}$ ) was used as a positive control (Liu et al., 2021). None of the OG treatments altered fresh weight, root length, and first leaf length. Conversely, CHIT strongly inhibited all growth-related parameters considered in a dose-dependent

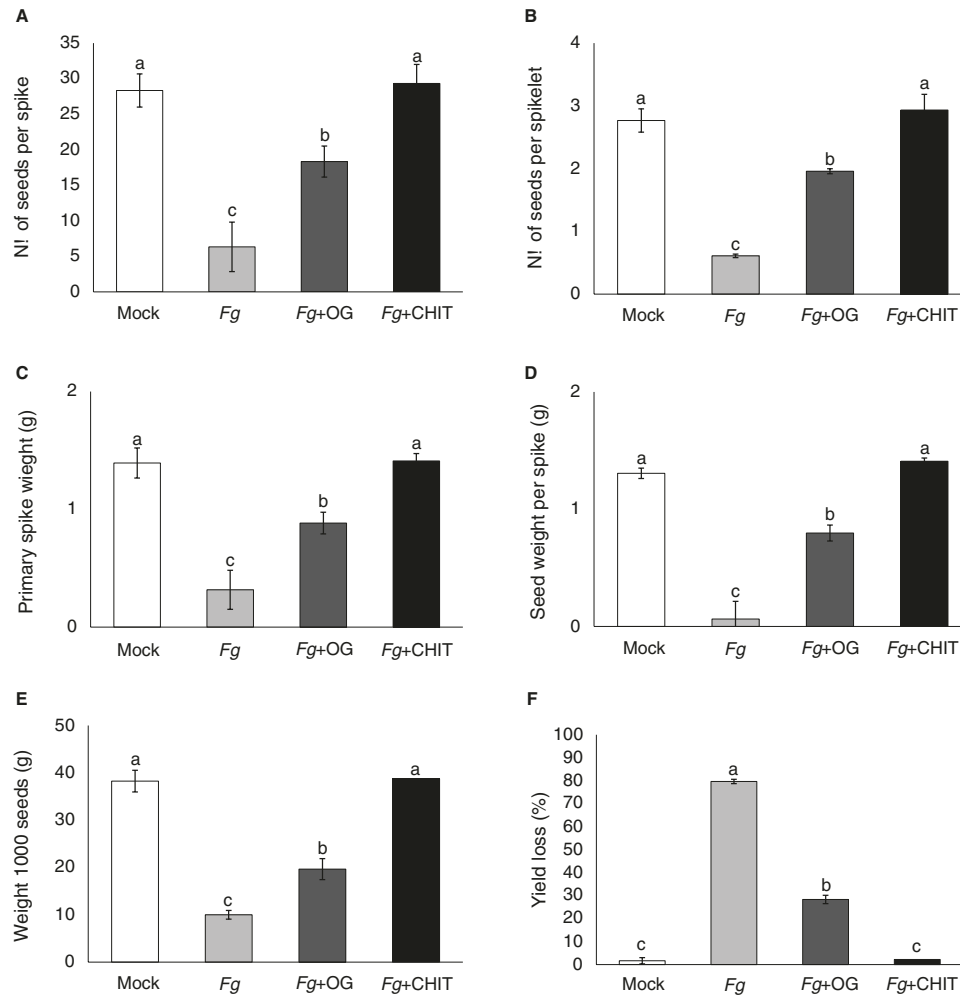


**Fig. 2.** Agronomic and growth parameters in OG- and CHIT-co-treated wheat plants after *F. graminearum* infection. Number of seeds per spike (A), number of seeds per spikelet (B), primary spike weight (C), seed weight per spike (D), weight of 1000 seeds (E), and yield loss (F) for the wheat cv. Svevo. A minimum of 10 plants per treatment condition were analysed to obtain data. All values are means  $\pm$  standard error (SE). The statistical significance was determined using ANOVA followed by Tukey test. Different letters indicate statistically different values ( $P < 0.05$ ).

manner (Fig. 4A–C). Indeed, in the presence of CHIT 100  $\mu\text{g ml}^{-1}$ , seedling fresh weight, root length, and first leaf length were inhibited by 57.4%, 83.2%, and 29.7%, respectively.

To evaluate the functionality of OGs as elicitors of immunity and their ability to restrict phytopathogen fungal growth also in durum wheat coleoptiles, 3-day-old seedlings were inoculated either with OGs at different concentrations (10, 100, or 500  $\mu\text{g ml}^{-1}$ ), *Fg* spores ( $2 \times 10^3$  conidia), or a co-treatment of both OGs and fungus spores. Sterile water was used as mock treatment and CHIT (2, 20, or 100  $\mu\text{g ml}^{-1}$ ) as a positive control in the experimental set-up. In the presence of co-treatments with both OGs or CHIT and the spores, disease lesion size and fungal accumulation, evaluated at different dpi, were significantly lower compared with seedlings treated with the fungus spores only (Fig. 5A–C). At 7 dpi, seedlings co-treated with OG 10, 100, and 500  $\mu\text{g ml}^{-1}$  showed a significant disease lesion size reduction of 14.8%, 41.8%, and 45.3%,

respectively. Seedlings inoculated with both CHIT and *Fg* displayed a reduction of 60.6% compared with seedlings treated with the fungus alone. It is worth noting that OGs triggered resistance to FHB in a dose-dependent manner, with the higher OG concentration used displaying the greater reduction in symptoms as well as in fungal accumulation. Indeed, in the presence of OG 10, 100, and 500  $\mu\text{g ml}^{-1}$ , the fungal amount was decreased by 30.4%, 35.7%, and 58.6% compared with seedlings treated with the fungus alone, whereas co-treatment with CHIT and *Fg* restricted the fungal amount by 84% (Fig. 5B).

To evaluate possible OG-dependent direct effects on fungal germination and/or growth we inoculated *Fg* spores in PDA plates containing different amounts (10 or 500  $\mu\text{g ml}^{-1}$ ) of OGs. CHIT (2, 20, or 100  $\mu\text{g ml}^{-1}$ ) was used as a positive control. Measurements of the fungal radial growth showed an inhibitory effect of both pectin fragment amounts on *Fusarium*

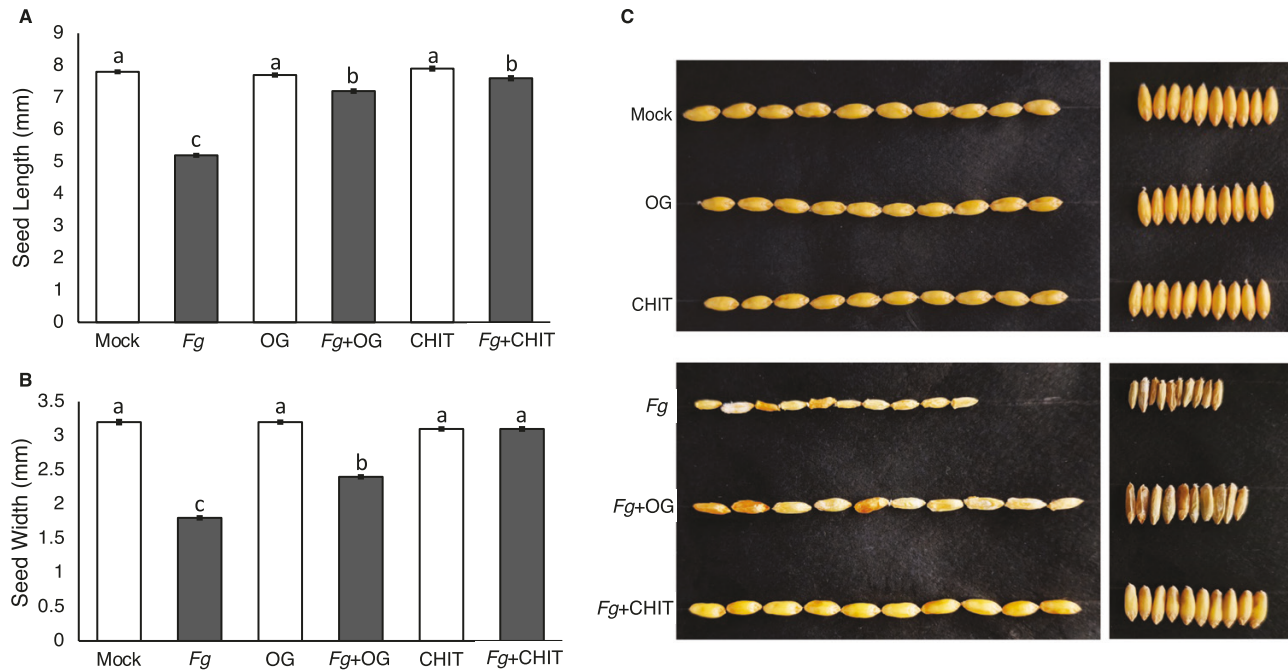


**Fig. 3.** Seed quality and filling in OG- and CHIT-co-treated wheat plants after *F. graminearum* infection. (A) Seed length. (B) Seed width. (C) Images showing length and width of representative seeds for each treatment condition. Ten seeds per treatment were analysed to obtain data. All values are means  $\pm$ SE. The statistical significance was determined using ANOVA followed by Tukey test. Different letters indicate statistically different values ( $P < 0.05$ ).

hyphal growth, similar to what was detected in CHIT-containing plates (Supplementary Fig. S2).

To ascertain the OG capability of activating systemic immune responses capable of restricting *Fusarium* colonization of wheat tissues, we germinated and grew wheat seedlings on half MS medium containing 10, 100, or 500  $\mu\text{g ml}^{-1}$  OGs for 3 d before inoculating *Fg* spores ( $2 \times 10^3$  conidia) in coleoptiles. As in the case of CHIT (2, 20, or 100  $\mu\text{g ml}^{-1}$ ), used as control, seedlings treated with all doses of OGs considered were able to induce higher resistance to *Fg* (Fig. 5A–D).

#### Transcriptome changes in elicited durum wheat seedlings infected with *F. graminearum*

Given the high similarity between the results obtained in spikes and seedlings infected with *Fg*, and to obtain a higher grade of reproducibility, the protocol published by Jia et al. (2017) for large-scale analyses has been adopted. RNAseq was carried out to obtain a general view of the transcriptome in durum wheat seedlings inoculated with OGs at different concentrations (10 and 500  $\mu\text{g ml}^{-1}$ ), *Fg* spores ( $2 \times 10^3$  conidia), or a co-treatment of both OGs and fungal spores for 48 h. Sterile water was used as mock treatment (control) and CHIT (100  $\mu\text{g ml}^{-1}$ ) as a well-established priming agent in the experimental set-up.

Sequencing of RNA samples produced an average of 36 994 174 reads per sample (ranging from 24 463 053 to 55 619 350; Supplementary Table S2). Reads mapped to the

durum wheat transcriptome using Salmon showed an average mapping rate of 78.67% (ranging from 67.26% to 88.34%). Total wheat read counts are reported in Supplementary Table S3. The data distribution is evident by observing results from a principal component analysis. The principal component analysis of count data showed that RNA samples of *Fg*-inoculated plants clustered far from the uninoculated ones, except for samples of plants inoculated with *Fg*+CHIT100 (Supplementary Fig. S3A), which grouped between the two groups. A limited variability was observed for samples of uninoculated plants (Supplementary Fig. S3B), while biological replicates of plants affected by the pathogen were slightly dispersed, considering *Fg* and *Fg*+OG treatments (Supplementary Fig. S3C). Conversely, *Fg*+CHIT100 replicates grouped separately (Supplementary Fig. S3C). A total of 4345 genes (out of 66073 *Triticum turgidum* subsp. *durum* total genes) were found to be differentially regulated in all samples. The DEGs compared with the control condition (mock) and identified in the diversely treated wheat coleoptiles are reported in Supplementary Tables S4–S12.

Considering the total up- and down-regulated genes (Supplementary Table S4), the treatment with most up-regulated genes was *Fg*+OG500 (2728 out of 2906 regulated genes) while the treatment with most down-regulated genes was *Fg* (494 out of 3214 regulated genes). The expression of a high number of genes was reprogrammed by the presence of the pathogenic fungus (Fig. S6A–C; Supplementary Table S4). The gene expression patterns of treatments without *Fg*, depicted

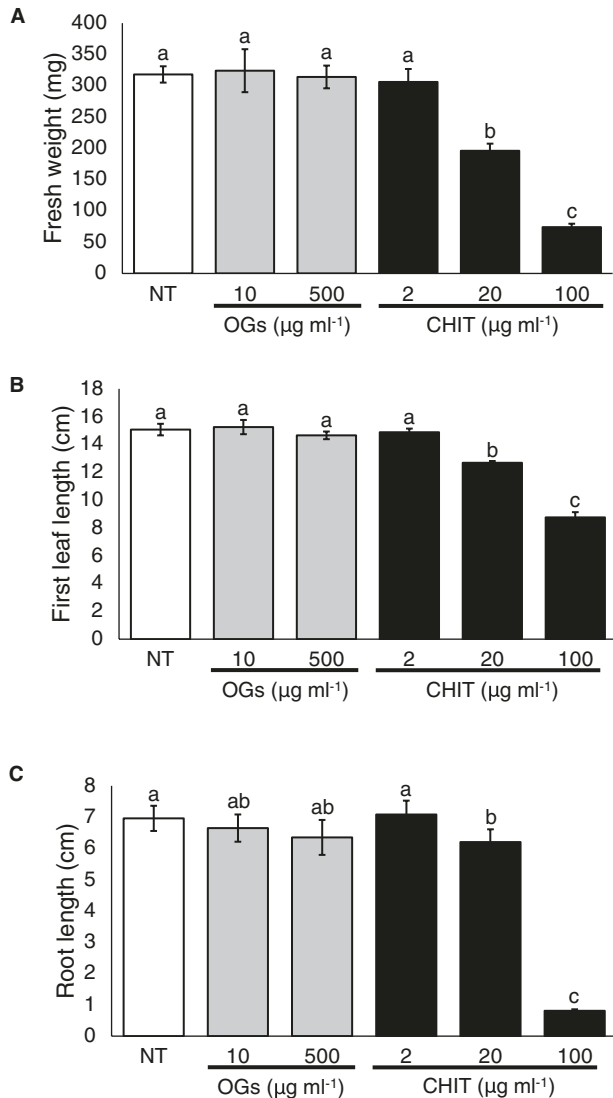


**Fig. 4.** Effects on morphological parameters of wheat seedlings grown in MS medium in the absence or presence of different concentrations of purified OGs or CHIT. (A) Fresh weight. (B) Root length. (C) First leaf length. The measurements were carried out 7 d after transplanting in MS medium. The statistical significance was determined using ANOVA followed by Tukey test. Different letters indicate statistically different values ( $P < 0.05$ ).

in [Supplementary Fig. S4](#), revealed a modest transcriptional remodeling in plants subjected to elicitors. Notably, the treatment involving CHIT100 exhibited dissimilar gene expression patterns compared with the two OG treatments. Additionally, while there was some overlap in the DEGs between the two OG treatments, distinct transcriptomic profiles were evident. Looking at the three immune elicitor treatments (OG10, OG500, and CHIT100), 84 genes were found to be exclusively regulated in OG10, 84 in OG500, and 133 in CHIT100 ([Supplementary Fig. S4](#)) compared with mock condition. A total of 13 DEGs were shared among the three different treatments in uninoculated plants ([Supplementary Table S13](#)).

The heatmap in [Fig. 6](#) reports the whole transcriptomic reprogramming in seedlings inoculated with *Fg* compared with the mock control condition, with and without immune elicitors, and shows that *Fg* and *Fg*+OG500 treatments exhibited similar patterns in terms of DEGs. On the other hand, the treatment *Fg*+OG10 appeared to have a distinct pattern compared with the other treatments, likely hinting at the activation of distinct signaling regulators and/or mechanisms. Particularly, *Fg*+OG10 is the treatment with the highest number of exclusive up-regulated genes (360 versus 220 in *Fg* as well as in *Fg*+OG500, and 78 in CHIT100) ([Fig. 6](#)). Moreover, *Fg*+CHIT100 showed a reduced number of DEGs compared with the other treatments. This might be due to the inhibitory effect of chitosan on *Fusarium* spore germination and to a consequent minor amount of plant cells challenged. In the presence of the phytopathogen fungus, only six genes were found to be commonly regulated between the elicitor co-treatments, including a hexokinase (TRITD1Bv1G065190), an auxin responsive gene (SAUR 36-like, TRITD5Av1G189370), a transcription factor (WRKY19-like, TRITD2Av1G050640), a mannose/glucose-specific lectin-like protein (TRITD4Av1G248450), a photosystem II phosphoprotein (TRITD1Bv1G023480), and an exocyst complex component (EXO70B1, TRITD0Uv1G091020) ([Fig. 6](#); [Supplementary Table S14](#)).

Infection marker genes, such as pathogenesis-related (*PR*) genes ([Supplementary Table S15](#)), were up-regulated in all the *Fg*-treated samples. The expression of 12 *PR1* genes, among the 24 paralogs in the durum wheat genome, was differently regulated in the different treatments, with some differences among them. Particularly, only one gene (TRITD5Bv1G112400) was significantly up-regulated in *Fg*+CHIT100 ( $\log_2FC = 5.69$ ), while all the *PR1* set was regulated with a  $\log_2FC$  average of 7.40, 5.22, and 7.61 in *Fg*, *Fg*+OG10, and *Fg*+OG500, respectively ([Supplementary Table S15](#)). Significant differences among average expression values of *PR1* genes in the four different treatments (*Fg*, *Fg*+OG10, *Fg*+OG500, and *Fg*+CHIT100) were detected. *PR1* expression was significantly higher in *Fg*, *Fg*+OG500, and *Fg*+OG10 compared with *Fg*+CHIT100 ( $P < 0.0001$ ), and in *Fg*+OG500 compared with *Fg*+OG10 ( $P = 0.040$ ). Although no significant differences were detected between *Fg* and *Fg*+OG500 expression values ( $P = 0.9944$ ), *PR1* expression in *Fg*+OG500 was slightly higher compared with *Fg* (7.61 versus 7.40). Considering the down-regulated genes, no gene was commonly down-regulated between *Fg*+OG10 and *Fg*+OG500, whereas the highest number of exclusive down-regulated genes was found in *Fg* (318) followed by *Fg*+OG10 (184), *Fg*+OG500 (75), and *Fg*+CHIT100 (57) ([Fig. 6C](#)).

Shared and exclusive DEGs were found among *Fg*, *Fg*+OG500, displaying the highest OG-induced resistance in the pathogenicity assays, and OG500 alone ([Fig. 7](#)). Among the 113 DEGs in OG500 ([Supplementary Table S4](#)), 47 were exclusive, while

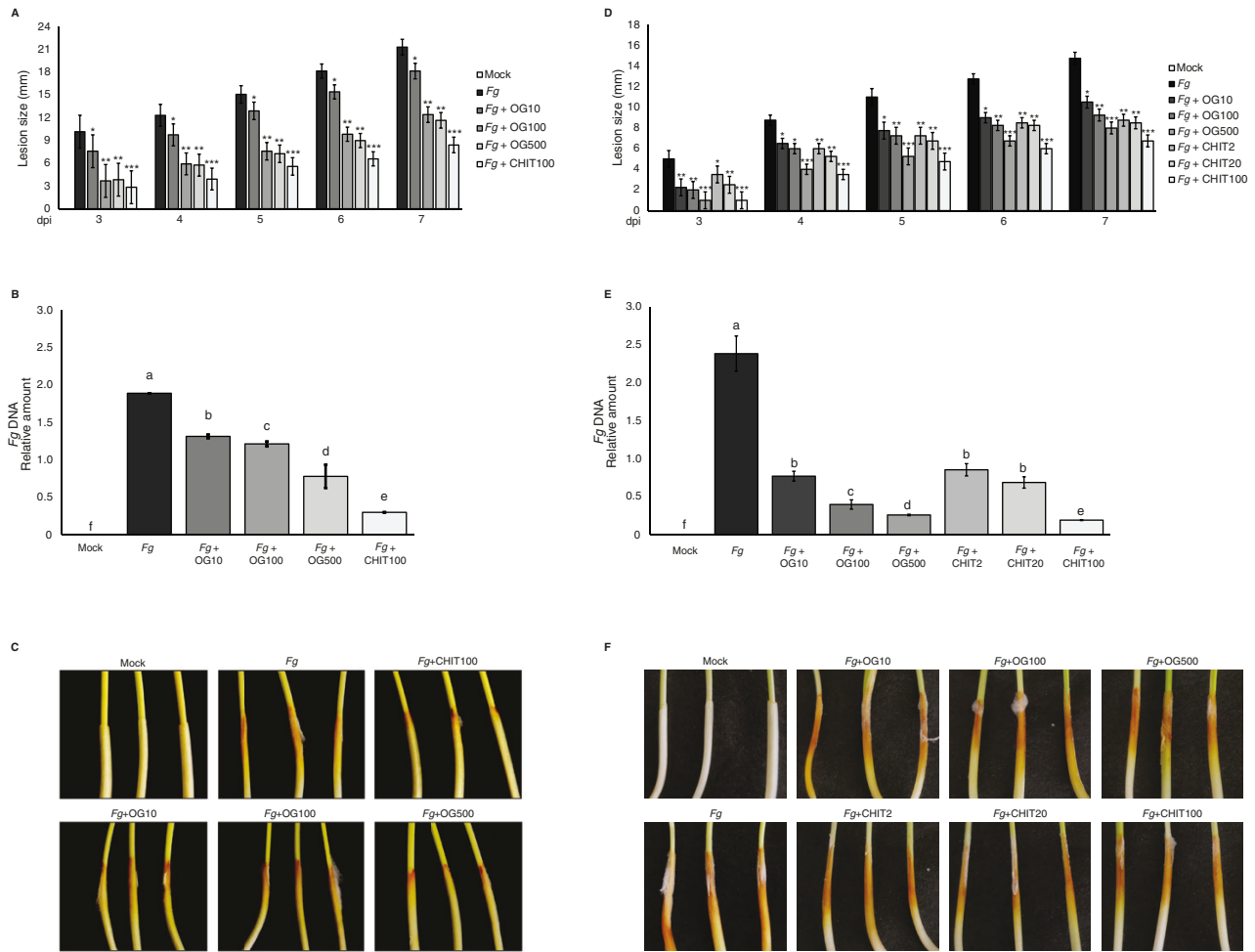


**Fig. 5.** Oligogalacturonides (OGs) trigger local and systemic resistance to *Fusarium* head blight in a dose-dependent manner. (A, D) Coleoptile lesion size in Svevo seedlings locally co-treated with *Fg*, *Fg*+OGs [at the indicated amounts ( $\mu\text{g ml}^{-1}$ )], or *Fg*+CHIT (A) or grown in the absence or presence of the indicated amounts of elicitors for 3 d and then inoculated with *Fg* spores (D). Disease symptoms were monitored for 7 days post inoculation (dpi). (B, E) Fungal genomic DNA quantification by real-time PCR analyses of the *Fg*  $\beta$ -*tubulin* gene normalized to the wheat *TdACTIN* gene in wheat coleoptiles at 7 dpi. (C, F) Images taken at 7 dpi showing disease spread in representative wheat coleoptiles for each treatment condition. All values are means  $\pm$ SE ( $n=10$ ). Asterisks above the bars indicate values that are significantly different from seedlings inoculated with the *Fg* alone ( $*P<0.05$ ,  $**P<0.01$ ,  $***P<0.001$ , Student's *t*-test).

62 were in common with *Fg* and *Fg*+OG500, although with a different expression level (59 up-regulated in the three treatments and three down-regulated in OG500 and up-regulated in *Fg* and *Fg*+OG500; [Supplementary Table S2](#)). Comparing the expression of these genes in OG10 and *Fg*+OG10, it was evident that a diverse regulation occurred ([Supplementary Fig. S5](#)), suggesting that a threshold effect due to the different OG concentrations could explain the difference in transcriptome profile. Several commonly regulated DEGs in these conditions encode transcription factors belonging to diverse groups as well as defense-related proteins ([Fig. 8](#)). Indeed, in agreement with [Kazan and Gardiner \(2018\)](#), the presence of *Fg* triggered the expression of genes involved in signaling and defense, cell wall remodeling, phenylpropanoid/lignin metabolism (e.g. endoglucanases, laccases), transport (e.g. ABC transporters), chitinases,

and glucan endo-1,3- $\beta$ -glucosidases (1,3-glucanases). Although several genes regulated in response to *Fg* infection showed a similar trend in both OG treatments, 295 and 544 genes were only regulated in *Fg*+OG10 or *Fg*+OG500, respectively, and others presented a diverse regulation in *Fg*+OG10 and *Fg*+OG500 ([Fig. 6](#); [Supplementary Table S11](#)). The top five genes found to be up-regulated only after the *Fg*+OG500 treatment encode for a probable LRR receptor-like serine/threonine-protein kinase ( $\log_2\text{FC}=7.39$ ; TRITD0Uv1G107190), a scopoletin glucosyltransferase-like ( $\log_2\text{FC}=6.91$ ; TRITD2Av1G260470), a PLAT domain-containing protein 3 ( $\log_2\text{FC}=6.56$ ; TRITD2Av1G287330), a peroxidase 2-like ( $\log_2\text{FC}=6.37$ ; TRITD0Uv1G142450), and a glucan endo-1,3- $\beta$ -glucosidase GII-like ( $\log_2\text{FC}=6.29$ ; TRITD3Bv1G259660). Moreover, two putative glycerol-3-phosphate transporter 1

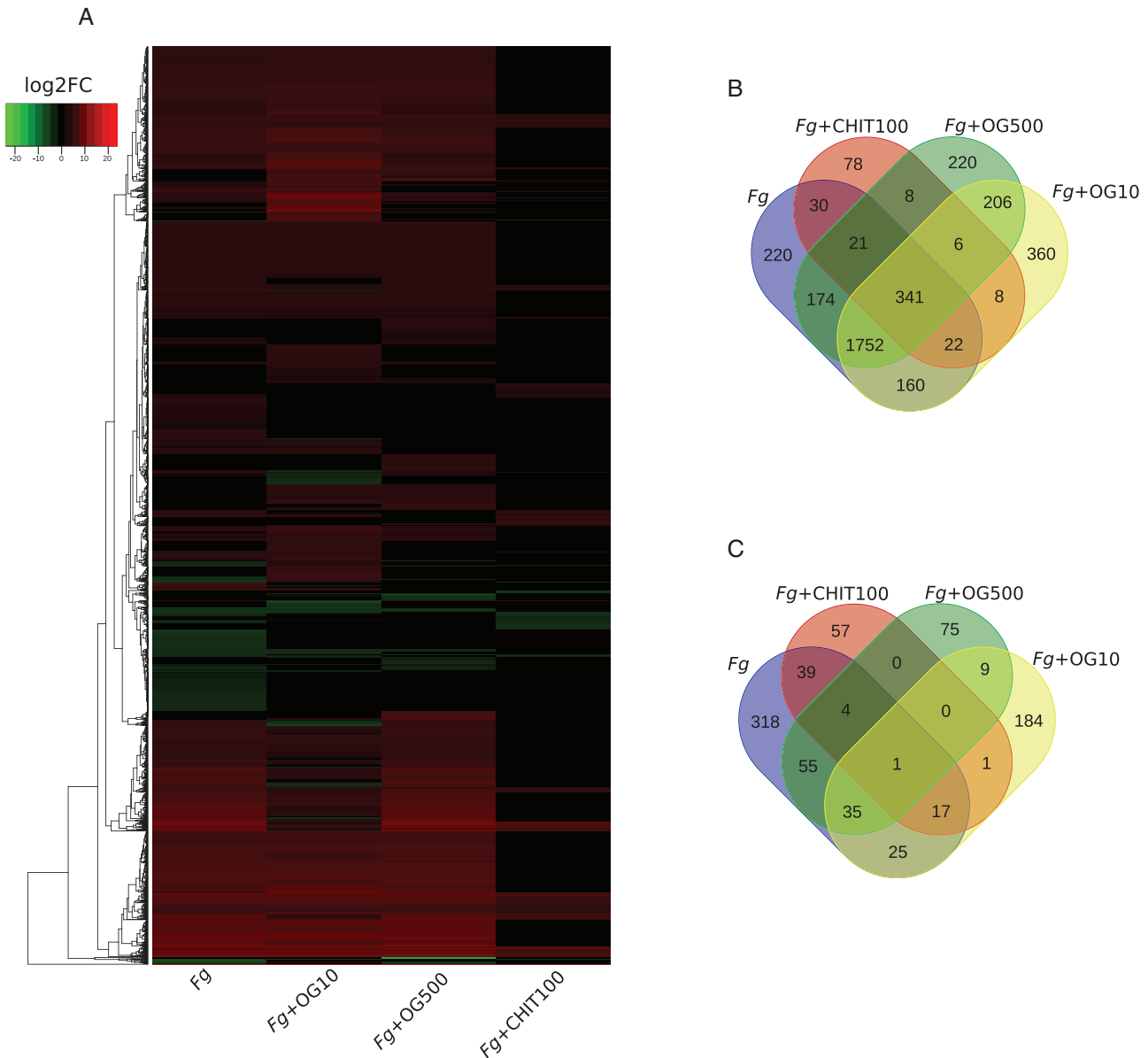


**Fig. 6.** Heatmap and Venn diagrams depicting DEGs in the conditions *Fg*, *Fg*+OG10, *Fg*+OG500, and *Fg*+CHIT100 versus control condition (mock). (A) Heatmap and hierarchical clustering of DEGs using the McQuitty algorithm. The heatmap shows the expression patterns of DEGs across four conditions compared with control (mock), with red levels indicating up-regulated and green representing down-regulated DEGs. Different color intensity indicates different levels of expression (log<sub>2</sub>fold change). (B, C) Venn diagrams illustrating the overlap of up- and down-regulated DEGs, respectively, between pairwise comparisons of the treatments.

(TRITD2Av1G242680 and TRITD2Bv1G203230), a known mobile regulator of systemic acquired resistance (Chanda *et al.*, 2011), were up-regulated in *Fg*+OG500. Fungal cell wall degrading enzymes, such as chitinases, were also found to be up-regulated after the pathogen infection in the presence of the OG treatments (Supplementary Table S12). One chitinase encoding gene (TRITD7Av1G248080) was up-regulated in OG10 and OG500 treatments in the absence of the pathogen as well. Gene expression data obtained by RT-qPCR analysis of 11 selected DEGs showed a significant degree of correlation with data

obtained with RNA-seq analysis ( $R^2=0.711$ ,  $P=2.503 \times 10^{-14}$ ; Supplementary Fig. S6; Supplementary Table S16).

#### GO enrichment analysis

To get an overview of the regulation of the main metabolic processes and signaling pathways involved in the different comparisons, we conducted GO enrichment analysis.

Differentially expressed transcripts were grouped in functional classes, based on the specific biological process in which

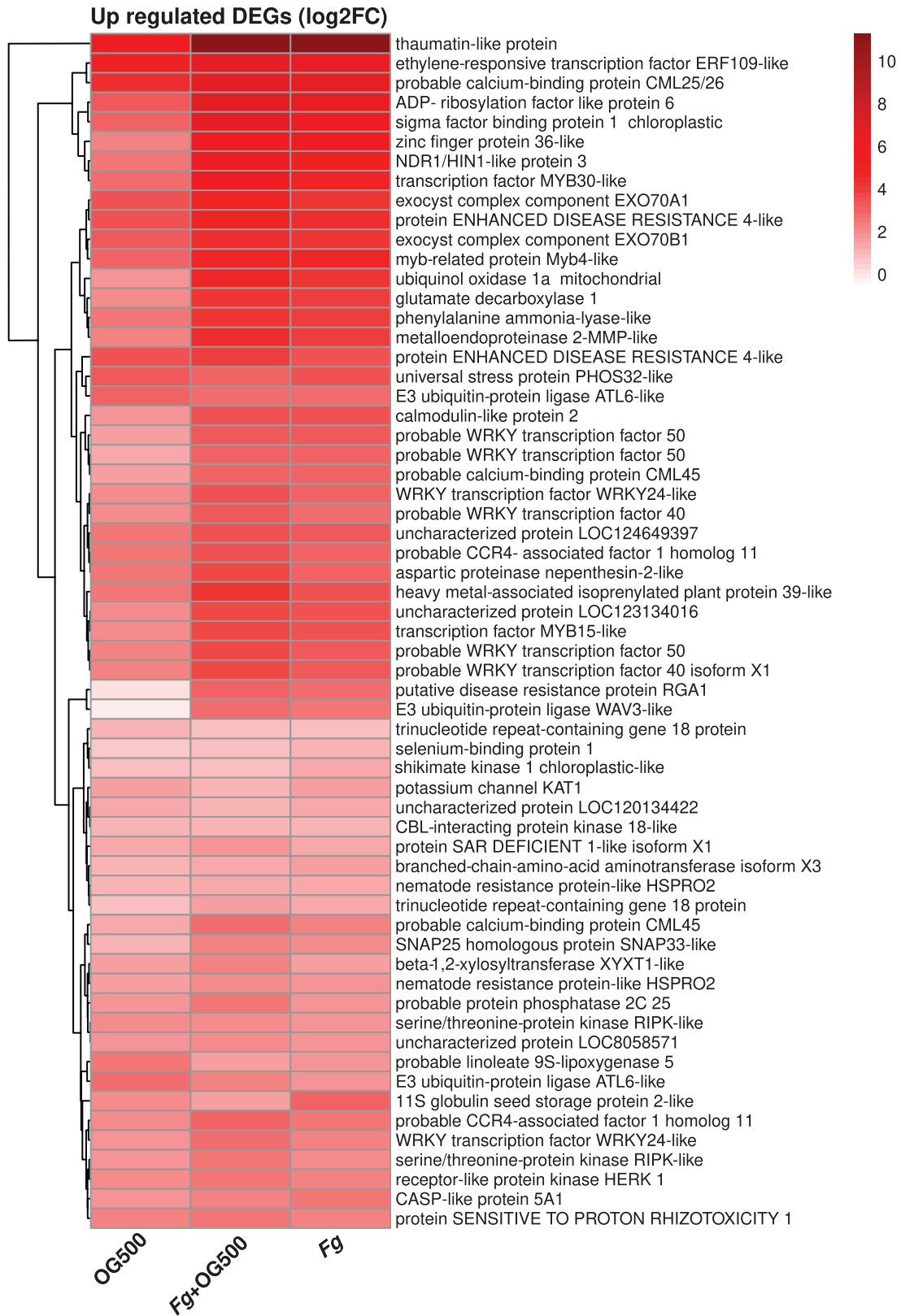


**Fig. 7.** Heatmap depicting expression of 59 up-regulated DEGs shared by condition *Fg*, *Fg*+OG500, and OG500. These shared DEGs may be related to a common response mediated by *Fg* and OG 500  $\mu\text{g ml}^{-1}$ . Different color intensity indicates different levels of expression (log2FC).

they are involved (Supplementary Table S17; Supplementary Figs S8, S9). Relevant terms found in OG10 transcriptome are ‘cellular oxidant detoxification’ and ‘detoxification’ (Fig. 8A), whereas, in OG500 different defense related processes were identified such as ‘lignin metabolic process’, ‘chitin catabolic process’, and ‘L-phenylalanine metabolic process’ (Fig. 8B). Results showed the presence in CHIT100 of different significant terms (false discovery rate <0.05) including those related to detoxification and amino acid metabolism (Fig. 8C). Significant GO terms found for transcripts in *Fg*-treated samples included chitin catabolism, phosphorylation, defense, response to oxidative stress, and amino acid metabolism (Fig. 9A). Conversely, the OG10 co-treatment with the fungus (*Fg*+OG10) led to transcript enrichment mainly related to the ‘glutathione metabolic process’, one of the most significant terms also identified in *Fg*+OG500 samples (Fig. 9B, C) together with ‘cell wall catabolic process’. As regards *Fg*+CHIT100, results showed the presence of different terms related to sulfur and amino acid metabolism, as in the case of CHIT100 (Fig. 9D).

#### *Transcriptome reprogramming by immunogenic signals in durum wheat seedlings*

Considering the effects of the OG10, OG500, and CHIT100 treatments in uninfected plants, 12 genes have been found to be commonly up-regulated (Supplementary Fig. S4; Supplementary Table S13), including genes encoding proteins previously reported to be involved in plant resistance to biotic stress in cereals, such as a CASP-like protein, two probable linoleate 9S-lipoxygenases 5 and Bowman-Birk type trypsin inhibitor like (Bhat *et al.*, 2019). Other up-regulated genes encoded a thaumatin-like protein (TRITD6Bv1G225300), also found among the up-regulated genes in *Fg* treatment, followed by an ethylene-responsive transcription factor (ERF109-like, TRITD1Bv1G202640) and a probable calcium-binding protein (CML25/26, TRITD4Av1G142800). Nevertheless, the two OG treatments exhibited dissimilar gene expression patterns compared with CHIT100 and, importantly, distinct transcriptomic profiles were also evident between treatments with OG10 and OG500 (Supplementary Fig. S4). Indeed, 65 genes were found to be exclusively regulated in OG10, 71 in OG500, and 52 in CHIT100 (Supplementary Fig. S4B). The most up-regulated gene in all the treatments was a *peroxidase 5 like* gene (TRITD0Uv1G116360), with the only exception being the OG500 treatment, although a high variability was observed among the biological replicates. Variability among biological replicate read counts of this gene may indicate that the observed difference can be influenced by technical and biological variation of the experiment. However, since the LFC effect size estimator was used during DESeq2 analysis, and the *P*-adjusted value is lower than the threshold ( $P < 0.05$ ), the difference in expression could be the result of a true biological difference. Additionally, no reads corresponding to this transcript have been found in the OG500 treatment in any

replicates (Supplementary Table S3). An individual variability was observed for several transcripts suggesting that expression for these genes might be very specific in timing and tissue localization. Despite the standardization in OG application and infection procedure, a seedling variability in the individual response might occur as already reported by Sorrentino *et al.* (2021).

Among the 71 exclusive up-regulated genes identified in OG500-treated tissues ( $P_{adj} < 0.05$ ), several genes are involved in signaling and plant response to biotic stresses. In particular these encoded a putative polyamine oxidase-like (log2FC=3.087; TRITD7Av1G204550), a homeobox-leucine zipper protein (log2FC=2.86; TRITD2Bv1G191820), a mannose/glucose-specific lectin-like (log2FC=2.87; TRITD4Av1G248390), two GDSL esterase/lipase proteins (log2FC=2.67; TRITD0Uv1G053990; log2FC=0.72; TRITD4Bv1G060640), a dirigent protein (log2FC=2.29; TRITD0Uv1G010390), an auxin-responsive protein (SAUR36-like, log2FC=1.74; TRITD5Av1G189140), a probable apyrase (log2FC=1.17; TRITD4Bv1G199760), a germin-like protein (log2FC=1.12; TRITD6Bv1G216490), a NDR1/HIN1-like protein (log2FC=0.76; TRITD3Bv1G120400), and a non-specific lipid-transfer protein (log2FC=0.72; TRITD2Bv1G226450). Moreover, genes coding for serine/threonine-protein kinases (TRITD0Uv1G123990, TRITD1Av1G199560, TRITD2Av1G294740) were specifically and significantly down-regulated in addition to a putative class II heat shock protein (TRITD3Bv1G044290), a calmodulin-binding transcription factor activator (TRITD2Bv1G141170), a transcription factor VOZ-1 like (TRITD1Bv1G186320) and a 3-hydroxyacyl-CoA dehydratase gene (TRITD3Bv1G024940).

#### *Oligogalacturonide-dependent regulation of genes putatively involved in immune signaling and plant cell wall remodeling in durum wheat seedlings*

Homologous genes of known important modulators of immune responses in plants were identified as DEGs through the transcriptomic analyses. Intriguingly, genes potentially involved in OG sensing and homeostasis, such as wall-associated receptor kinases (Wan *et al.*, 2021) and members of Berberine-Bridge Enzyme-like (BBE-I) family (Benedetti *et al.*, 2018; Locci *et al.*, 2019; Pontiggia *et al.*, 2020), were up-regulated (28 and 5 genes, respectively) during the infection, except in the *Fg*+CHIT100 co-treatment. Among the genes coding for the wall-associated receptor kinases, it is worth noting the presence of three genes exclusively regulated by OG500, i.e. TRITD2Av1G016690, which was down-regulated in *Fg*+OG500 (log2FC=-4.81), and TRITD5Bv1G188610 and TRITD6Bv1G224850, which conversely were up-regulated in the same condition (log2FC=1.05 and 5.76, respectively). Additionally, five genes belonging to the BBE-I family were differentially expressed in *Fg*, *Fg*+OG10, and *Fg*+OG500-treated

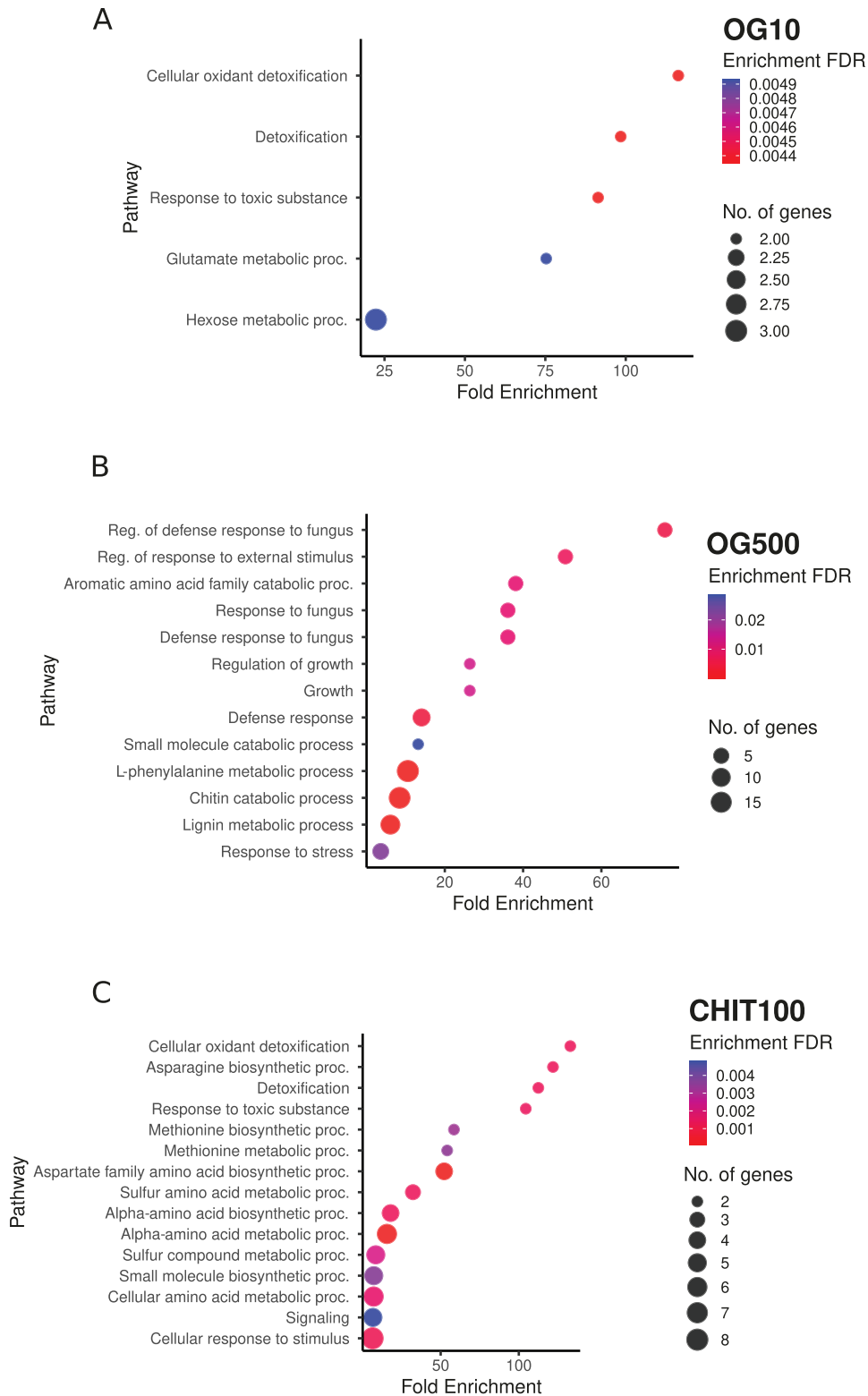


**Fig. 8.** Bubble plots showing GO-enriched terms classified as biological process (BP) in detected DEGs. In detail, enriched terms in OG10 (A), OG500 (B), and CHIT100 (C) are reported. The x-axis shows the fold enrichment values, i.e. the percentage of genes in the selected DEG list belonging to a pathway divided by the corresponding percentage in the all reference gene list, and the y-axis reports the GO terms. Sizes of bubbles are proportional to the number of genes assigned to the related GO term, while bubble color indicates the significance of the enriched term (false discovery rate (FDR) values) as calculated by the enrichment analysis by Blast2GO.

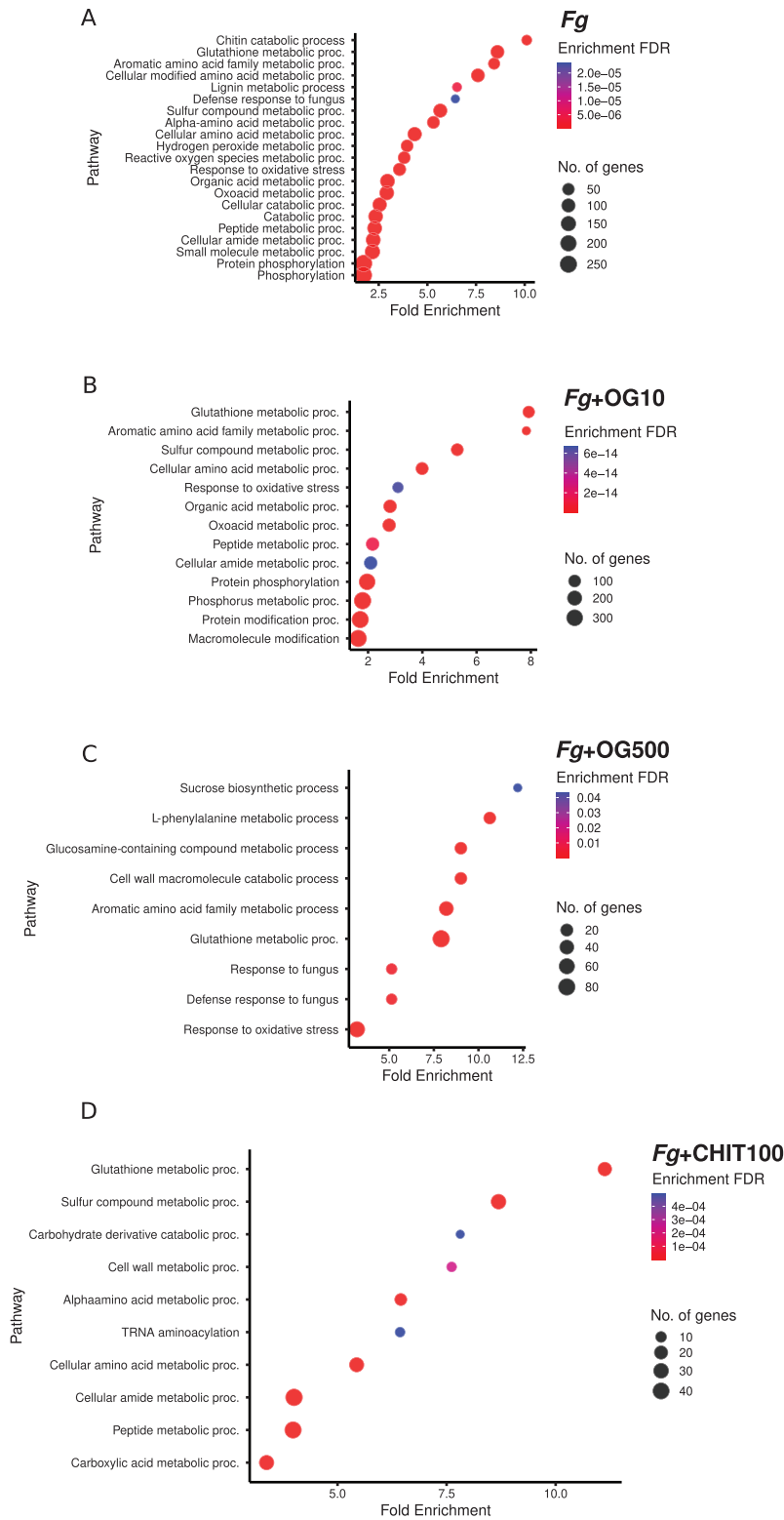


**Fig. 9.** Bubble plots showing GO-enriched terms classified as biological process (BP) in detected DEGs. In detail, enriched terms in *Fg* (A), *Fg+OG10* (B), *Fg+OG500* (C), and *Fg+CHIT100* (D) are reported. The x-axis shows the fold enrichment values, i.e. the percentage of genes in the selected DEG list belonging to a pathway divided by the corresponding percentage in the all reference gene list, and the y-axis reports the GO terms. Sizes of bubbles are proportional to the number of genes assigned to the related GO term, while bubble color indicates the significance of the enriched term (false discovery rate (FDR) values) as calculated by the enrichment analysis by Blast2GO.

seedlings compared with mock control condition, and three of them showed a stronger up-regulation in *Fg*+OG10 compared with other treatments (TRITD7Av1G190220, log<sub>2</sub>FC=10.85; TRITD7Bv1G154140, log<sub>2</sub>FC=7.74; TRITD5Av1G158460, log<sub>2</sub>FC=8.29) (Supplementary Table S12). Alignment of their protein sequences highlights marked similarity (>45%) to AtCELLOX1, which is involved in oxidation, and consequent inactivation, of cellodextrins, a well-known class of cell-wall-derived DAMPs (Souza *et al.*, 2017). Furthermore, Locci *et al.* (2019) observed that the oxidized cellodextrins are not a carbon source for the known pathogenic fungus *Botrytis cinerea* suggesting an indirect antimicrobial activity against pathogenic fungi. The ‘function’ of the five BBE-1 family-related genes (as the expression average value of all the genes putatively belonging to BBE-1 family), was not significantly different among *Fg*, *Fg*+OG10, and *Fg*+OG500 (ANOVA, *P*>0.05; average expression values  $3.49 \pm 1.32$ ,  $6.25 \pm 3.91$ , and  $3.57 \pm 1.28$ , respectively); however, when only TRITD7Av1G190220, TRITD7Bv1G154140, and TRITD5Av1G158460 were considered, their average expression was significantly higher in *Fg*+OG10 (average of  $8.96 \pm 1.66$ ) compared with that of *Fg* and *Fg*+OG500 ( $4.29 \pm 0.92$  and  $4.39 \pm 0.59$ , respectively; ANOVA, *P*<0.00001).

Similar behavior was also detected for cytosolic serine/threonine-protein kinase-encoding genes (e.g. *PBS-LIKE*, *PBLs*) and for the *ENHANCED DISEASE RESISTANCE4* (*EDR4*) gene. In Arabidopsis PBLs are important transducers of danger signals (Rao *et al.*, 2018) while *EDR4* modulates plant immunity by associating with clathrin and regulating the relocation of *EDR1* (Wu *et al.*, 2015) or by regulating the association of key signaling elements to inhibit cell death (Neubauer *et al.*, 2020). We found both *PBL* and *EDR1* paralogs to be up-regulated in all the infected samples, except *Fg*+CHIT100. Interestingly, *EDR1* was also up-regulated only in OG500 samples among those treated with elicitors of immunity. Another interesting hint regards the expression of *NPR1*, encoding a regulatory protein involved in the salicylic acid signaling pathway (Janda and Ruelland, 2015); it was found to be significantly overexpressed only in *Fg*+OG10 (log<sub>2</sub>FC=7.38), whereas, at the analysed hpi, the log<sub>2</sub>FC values for *Fg* and *Fg*+OG500 samples were 1.37 and 1.70, respectively.

As previously reported in Kazan and Gardiner (2018), several genes involved in plant cell wall synthesis and degradation were found to be regulated after *Fg* infection. Most of them were up-regulated in all the *Fg* infected plants (*Fg*, *Fg*+OG10, and *Fg*+OG500; Supplementary Table S12). Among them, genes coding for pectin-modifying enzymes such as a pectinesterase (TRITD1Bv1G117660) and three putative pectinesterase/pectinesterase inhibitors (TRITD1Av1G166830, TRITD5Bv1G222340, TRITD1Bv1G152660), involved in plant resistance to necrotrophs by regulating the pectin methyltransferase activity (Lionetti *et al.*, 2017), were commonly up-regulated in the three diverse co-treatments. It is worth noting that the two last (TRITD5Bv1G222340 and

TRITD1Bv1G152660) presented slightly higher log<sub>2</sub>FC values in *Fg*+OG treatments with respect to the *Fg* treatment. Moreover, a gene coding for a probable pectinesterase (TRITD2Av1G026410) and two genes coding for pectinesterase inhibitors (TRITD2Av1G261160, TRITD1Bv1G228800) were significantly up-regulated only in seedlings treated with OG10, whereas *Fg*+OG500-treated plants specifically displayed a higher expression of an endo-1,4-β-xylanase (TRITD5Av1G136370) and an α-1,3-arabinosyltransferase (TRITD6Av1G190480). The expression of six genes for endoglucanases, enzymes with a role in cell wall remodeling during pathogen infection, was found to be significantly up-regulated: two genes (TRITD1Av1G025050 and TRITD6Av1G192020) were expressed in *Fg*, *Fg*+OG10, and *Fg*+OG500-treated seedlings, while four genes were significantly up-regulated only in *Fg*+OG10. Several genes putatively involved in phenylpropanoid/lignin biosynthesis have been also identified as up-regulated after *Fg* infection (Supplementary Table S12). A different regulation in the two OG treatments was revealed considering the coumarate CoA ligase genes: seven genes were differently regulated and, worth noting, this ‘function’ (as the expression average value of all the genes belonging to this category) was differently up-regulated in the three conditions (0.33 in *Fg*, 2.80 in *Fg*+OG10, and 0.29 in *Fg*+OG500). A gene coding for a putative glycerol-3-phosphate acyltransferase (RAM2, TRITD4Av1G006510), reported to provide precursors for the synthesis of secreted lipids such as cutin, was down-regulated in plants infected by the pathogen, while it was not regulated in OG-treated plants. It has been demonstrated that RAM2 proteins are required for the establishment of a functional root symbiosis, as the corresponding loss-of-function mutants are impaired in the formation of fully developed arbuscules (Luginbuehl and Oldroyd, 2017). Genes coding for four epoxide hydrolases, which could be involved in the biosynthesis of polyhydroxylated cutin monomers, were found to be regulated in infected and OG co-treated plants, with differences in the expression correlated with the OG dose (Supplementary Table S12). Particularly, TRITD6Av1G005800 presented a log<sub>2</sub>FC value of 6.12 in *Fg*+OG500 versus a log<sub>2</sub>FC value of 1.37 in *Fg*+OG10. Genes coding for 3-ketoacyl-CoA synthases, reported as a negative regulator in cuticular wax production (Huang *et al.*, 2023), appeared to be significantly finely tuned in all the infected plants (Supplementary Table S12).

#### *Changes in F. graminearum transcriptome mediated by oligogalacturonides*

For each inoculated sample, an average of 14% of non-aligned reads to plant transcriptome were successfully aligned to available *Fg* transcriptome and ranged from 890 614 to 2 380 036 with an average of 1 527 554 (Supplementary Table S18). A very low percentage of reads aligned against fungal transcriptome for samples coming from infected plants treated with CHIT100 (approximately 0.02%; Supplementary Table S18).

Total fungal read counts are reported in [Supplementary Table S19](#). Identification of DEGs in *Fg* infecting durum wheat tissues upon treatment with OG500 revealed alterations in gene regulation, with a total of 61 genes showing differential expression compared with *Fg* in plants without co-treatment (38 up- and 23 down-regulated; [Supplementary Table S20](#)). On the other hand, only seven DEGs (three up- and four down-regulated) were found in the fungus in the presence of OG10 ([Supplementary Table S21](#)). Four genes (FGSG\_03061T0, FGSG\_03915T0, FGSG\_02477T0, and FGSG\_10675T0) were detected as DEGs in both conditions, with a similar expression pattern. Two genes encoding a putative NADH-dehydrogenase (ubiquinone) (FGSG\_02477T0) and an uncharacterized protein (FGSG\_10675T0) were up-regulated by the two OG treatments, while two genes putatively coding for a sorbitol dehydrogenase and a flavin-containing monooxygenase (FGSG\_03061T0 and FGSG\_03915T0, respectively) were down-regulated. One of the key factors contributing to the virulence of *Fg* is the production of mycotoxins, such as deoxynivalenol, whose synthesis involves genes collectively known as the *Tri* genes ([Jiang et al., 2016](#)). In *Fg*, *Fg*+OG10, and *Fg*+OG500, reads aligned with 13 *Tri* genes, but when compared with *Fg*, no significant differences were detected (DEGs showed  $P_{adj} > 0.05$ ) and, for this reason, they were not further considered ([Supplementary Table S22](#)).

## Discussion

The use of elicitors able to stimulate the plant innate immune system represents a novel and promising strategy in crop protection, as an alternative to conventional pesticides. OGs are potent elicitors of immunity when applied exogenously as they trigger a wide range of defense responses including accumulation of phytoalexins in soybean ([Davis et al., 1986](#)), deposition of callose, production of reactive oxygen species ([Galletti et al., 2008](#); [Gravino et al., 2017](#)) and nitric oxide (NO) ([Rasul et al., 2012](#)) in Arabidopsis, accumulation of salicylic acid in strawberry ([Osorio et al., 2008](#)), and activation of defense-related genes ([Denoux et al., 2008](#); [Gravino et al., 2017](#)). It is worth noting that a dose-dependency for some elicitors, including OG and Flg22, has been already reported in the induction of defense response pathway in Arabidopsis seedlings ([Denoux et al., 2008](#)). Nevertheless, a clear demonstration of the capability of OG to activate defense-associated responses and resistance to *Fg* in wheat is so far lacking. Here, when exogenously applied, OGs could restrict FHB symptoms in a dose-dependent manner both locally and systemically, therefore indicating that they are sensed as danger signals in different durum wheat tissues, i.e. spikes and cotyledons ([Figs 1, 5](#)). A slowed disease progression, accompanied by a lower amount of fungus, was detected in infected wheat spikes co-treated with OGs compared with the ears inoculated with the *Fg* alone ([Fig. 1](#)). Consequently, elicitor treatments positively

impacted the agronomic and yield parameters as well ([Fig. 2](#)). This study shows that exogenous application of OGs reduces the yield losses associated with FHB infection by 51% ([Fig. 2F](#)). Moreover, spikes co-treated with *Fg* and OGs displayed higher values compared with ears treated with the fungus alone in terms of number of seeds per spike and spikelet, primary spike weight, seed weight per spike, and weight of 1000 seeds ([Fig. 2A–E](#)). Furthermore, it was observed that OGs and chitosan limit the shriveling of *Fg*-infected durum wheat seeds ([Fig. 3](#)). Wheat spikes and seeds in *Fg*+CHIT100 co-treatment did not show differences compared with the untreated condition. Such a lack of disease symptoms could be explained by the capability of chitosan to inhibit fungal spore germination, mycelium growth, and virulence ([Francesconi et al., 2020](#); [Luan et al., 2022](#)). Interestingly, a similar, but lower, inhibitory direct effect on *Fg* growth was also detected by adding different amounts of OGs to the fungal growth medium, hinting that, locally, OGs may act not only as an elicitor of wheat immunity but also as a blocker of fungal growth. OGs and CHIT triggered resistance to *Fg* also in 3-day-old Svevo seedlings ([Fig. 5](#)). It is noteworthy that none of the OG doses considered in this study altered fresh weight, root length, and first leaf length compared with untreated plants ([Fig. 4](#)). Conversely, CHIT strongly inhibited all the biometric parameters, hinting that shared and distinctive responses are activated in response to the two oligosaccharins both locally and systemically.

To deeper understanding of the genetic bases of the observed durum wheat behavior in response to OGs and CHIT as well as the OG dose-dependency effect on wheat response both in the presence and the absence of *Fg*, RNAseq analyses were carried out, showing that OGs, as CHIT, act as elicitors of immune responses. Results showed that the transcriptome profiles of plants were differently remodeled not only depending on the basis of the applied elicitors but also depending on the applied concentrations. Additionally, results also revealed differences in fungal reads within the transcriptomic data. The infected plants without OG treatment exhibited an increase in fungal reads, suggesting a high presence of *Fg*-related genetic material, while plants infected and co-treated with OG500 and OG10 displayed a reduction in fungal reads. This suggests that the application of OGs effectively slowed the fungal infection, resulting in a decreased abundance of *Fusarium*-related genetic material, also confirmed by fungal DNA quantification through qPCRs. In agreement with previous published data on wheat response to pathogens ([Anguelova-Merhar et al., 2001](#); [Tripathi et al., 2013](#); [Zhang et al., 2019](#)), DEGs related to several defense genes, including those encoding chitinases and  $\beta$ -1,3-glucanases, were identified. It is worth noting that different genes encoding chitinases were found to be up-regulated in OG10-inoculated plants, while only one gene coding for a basic endochitinase-like (TRITD7Av1G248080) was up-regulated in OG500-treated seedlings, confirming the activation of different mechanisms depending on the OG concentration. Several genes have been differentially regulated

in OG10 treatment and OG500 treatment, suggesting that wheat cotyledons can sense and respond specifically to different amounts of OGs. The differences observed among the two OG treatments, either in the absence or in the presence of the pathogen, are also reflected by the GO enrichment profiles.

Among the genes exclusively up-regulated in OG500 treatment, a putative *polyamine oxidase-like* was found. It has been suggested that the production of hydrogen peroxide (H<sub>2</sub>O<sub>2</sub>) deriving from polyamine oxidation might be correlated with cell wall reinforcement during pathogen invasion, besides cell wall maturation and lignification during plant development. The H<sub>2</sub>O<sub>2</sub> originated from polyamine oxidation may be involved as a signal molecule in mediating cell death, the hypersensitive response, and expression of defense genes (Cona *et al.*, 2006), and recently has been shown to be involved in systemic wound-triggered stomatal closure (Fraudentali *et al.*, 2023). Further, both *EDR4* and *NHL* genes, involved in the activation of plant defense responses to biotic stresses (Maldonado *et al.*, 2014; Chen *et al.*, 2018), were found to be up-regulated in response to OG500, confirming the regulation of defense-related genes mediated by these elicitors, independently from the presence of the pathogen. Expression of genes involved in plant cell wall metabolism was also altered, including genes involved in the phenylpropanoid pathway. Among them are genes encoding caffeoylshikimate esterase (CSE)-like, involved in lignin biosynthesis (Vanholme *et al.*, 2013). A CSE has been recently reported to be involved in mediating the cucumber disease resistance to a fungal attack by promoting lignin biosynthesis (Yu *et al.*, 2022). In our experiment, four genes were up-regulated in *Fg* and *Fg*+OG500, while only two appeared to be up-regulated in *Fg*+OG10 treatments. Also, expansins, involved in plant cell wall remodeling (Cosgrove, 2000), were specifically regulated by OGs, in the presence or absence of *Fg*, whereas, noteworthy, none was significantly regulated by CHIT. A similar expression pattern was observed for genes related with OG sensing and homeostasis, i.e. cell wall-associated kinases and BBE-I. Particularly, five genes correlated to BBE-I were up-regulated by the two doses of OGs in the presence of the fungus.

On the other hand, in *Fg*, upon OG500 treatment, the down-regulation of fungal genes related to energy production and conversion, lipid transport and metabolism, replication, carbohydrate transport and metabolism, and amino acid metabolism suggested potential changes in various fungal cellular processes. It could be hypothesized that these changes may have implications for the fungal growth and interactions with the plant host. The up-regulation of *NADH-dehydrogenase* in *Fg* in plants treated either with OG10 or OG500 may suggest a protective role against oxidative stress. Previous studies have provided evidence that alternative NADH dehydrogenases in filamentous fungi exhibit increased activity in the presence of oxidative stress (Bai *et al.*, 2003; Voulgaris *et al.*, 2012).

Moreover, down-regulation of a putative fungal flavin-containing monooxygenase was found in both conditions with OGs. Flavin-containing monooxygenases have a broad

distribution across different organisms and play diverse roles in various biological processes, including detoxification (van Berkel *et al.*, 2006). It could be hypothesized that down-regulation of a flavin-containing monooxygenase genes can affect fungal detoxification mechanisms, resulting in a reduced detoxification capacity. The lack of significant differences in trichothecene biosynthetic gene (*Tri*) gene expression between *Fg*-infected with OG and *Fg*-infected plants may be explained by the possibility that the time point at which the samples were collected might not have captured the dynamic changes in *Tri* gene expression (Lee *et al.*, 2014). Additional time-course experiments with multiple sampling points would be beneficial in elucidating the temporal dynamics of *Tri* gene expression during *Fg* infection with and without OG application.

Overall, the transcriptomics data showed that specific plant responses were observed in the diverse treatments (different elicitors and doses), also in the absence of the fungal pathogen. Results demonstrated that OGs, like chitosan, limit the spread of the *Fg* in durum wheat plant tissues and, possibly, decrease the mycotoxin contamination and shed light on the functionality of OGs as elicitors of immunity and their ability in protecting a cereal like durum wheat, characterized by a high susceptibility to FHB. Exogenous application of OGs led to a significant decrease of FHB lesion sizes and diseased severity on wheat coleoptiles and spikes, respectively. This is the first observation of direct involvement of OGs in enhancing resistance to the *Fg* phytopathogen.

The improvement of natural plant defense mechanisms to control pathogen attacks is one of the most attractive strategies to increase resistance in a sustainable manner. In this scenario, the use of cell-wall-derived elicitors, such as OGs, able to stimulate the plant innate immune system, represents a novel and promising strategy in crop protection, as an alternative to conventional pesticides (Alexandersson *et al.*, 2016; Iriti and Varoni, 2017). Based on the knowledge that OGs may activate a wide range of defense responses, it will be of interest, in the near future, to generate and analyse durum wheat lines with altered capability in producing and/or sensing OGs.

## Supplementary data

The following supplementary data are available at [JXB online](#).

Fig. S1. OGs characterization.

Fig. S2. Elicitor-dependent *F. graminearum* radial growth inhibition.

Fig. S3. Principal components analysis (PCA) of normalized read counts (regularized log transformation of normalized data) of all samples used in RNAseq experiment.

Fig. S4. Heatmap and Venn diagrams representing DEGs in the conditions OG10, OG500, and CHIT100.

Fig. S5. Heatmap showing expression of 59 up-regulated DEGs depicted in Fig. 7.

Fig. S6. Correlation between RNA-seq data and RT-qCR results.

Table S1. List of selected plant genes and primers used in in the quantification by PCR analysis and RT-qPCR validation.

Table S2. Summary statistics of RNA-seq alignment of plant reads.

Table S3. Raw RNA-seq plant reads count.

Table S4. Number of up- and down-regulated DEGs in the seven different conditions.

Table S5. Significant ( $P_{\text{adj}} < 0.05$ ) DEGs in treatment OG10.

Table S6. Significant ( $P_{\text{adj}} < 0.05$ ) DEGs in treatment OG500.

Table S7. Significant ( $P_{\text{adj}} < 0.05$ ) DEGs in treatment CHIT100.

Table S8. Significant ( $P_{\text{adj}} < 0.05$ ) DEGs in treatment *Fg*.

Table S9. Significant ( $P_{\text{adj}} < 0.05$ ) DEGs in treatment *Fg*+OG10.

Table S10. Significant ( $P_{\text{adj}} < 0.05$ ) DEGs in treatment *Fg*+OG500.

Table S11. Significant ( $P_{\text{adj}} < 0.05$ ) DEGs in treatment *Fg*+CHIT100.

Table S12. Significant ( $P_{\text{adj}} < 0.05$ ) DEGs in the seven different conditions.

Table S13. Shared DEGs among the three treatments on uninoculated plants.

Table S14. Shared DEGs among *Fg*+OG10, *Fg*+OG500, *Fg*+CHIT100.

Table S15. *PR1* gene DEGs in conditions *Fg*, *Fg*+OG10, *Fg*+OG500, *Fg*+CHIT100.

Table S16. Gene expression data (log2FC) from RT-qPCR and RNA-seq of selected genes.

Table S17. GO enriched terms in the seven different conditions and associated genes.

Table S18. Summary statistics of RNA-seq alignment of fungal reads.

Table S19. Raw RNA-seq fungal reads count.

Table S20. Significant ( $P_{\text{adj}} < 0.05$ ) fungal DEGs in treatment *Fg*+OG500.

Table S21. Significant ( $P_{\text{adj}} < 0.05$ ) fungal DEGs in treatment *Fg*+OG10.

Table S22. Expression data of *Fusarium Tri* genes in *Fg*+OG500 and *Fg*+OG10.

## Author contributions

DVS and RB designed the experiments. VB performed pathogenic bioassays and analyses in spikes. VB and SG performed pathogenic bioassays and analyses in seedlings. FS and LG performed transcriptomic analyses. DP prepared OGs. DVS and RB prepared the article. VB and FS prepared the figures. All authors contributed to the article and approved the submitted version.

## Conflict of interest

Authors have no conflict of interest to declare.

## Funding

This study was carried out within the Agritech National Research Center and received funding from the European Union Next-Generation EU (PIANO NAZIONALE DI RIPRESA E RESILIENZA (PNRR) – MISSIONE 4 COMPONENTE 2, INVESTIMENTO 1.4 – D.D. 1032 17/06/2022, CN00000022) as well as in the framework of the Ministry for Education, University, and Research (MIUR) initiative "Department of Excellence" (Law 232/2016) DAFNE Project 2023–27 "Digital, Intelligent, Green and Sustainable (acronym: D.I.Ver.So)". The manuscript reflects only the authors' views and opinions, and neither the European Union nor the European Commission can be considered responsible for them. Transcriptomics and LG's fellowship were funded by the PRIMA project OPTIMUS PRIME (MUR DD 16302, 12/11/2021).

## Data availability

Data generated in this study are available in the supplementary data of this paper. RNA-seq reads were submitted to NCBI Sequence Read Archive (SRA) under BioProject accession number PRJNA977839.

## References

- Abdul Malik NA, Kumar IS, Nadarajah K.** 2020. Elicitor and receptor molecules: Orchestrators of plant defense and immunity. *International Journal of Molecular Sciences* **21**, 963.
- Alexandersson E, Mulugeta T, Lankinen A, Liljeroth E, Andreasson E.** 2016. Plant resistance inducers against pathogens in Solanaceae species—From molecular mechanisms to field application. *International Journal of Molecular Sciences* **17**, 1673.
- Alisaac E, Mahlein AK.** 2023. Fusarium head blight on wheat: biology, modern detection and diagnosis and integrated disease management. *Toxins* **15**, 192.
- Anguelova-Merhar VS, VanDer Westhuizen AJ, Pretorius ZA.** 2001. B-1,3-Glucanase and chitinase activities and the resistance response of wheat to leaf rust. *Journal of Phytopathology* **149**, 381–384.
- Aziz A, Trotel-Aziz P, Dhuciq L, Jeandet P, Couderchet M, Vernet G.** 2006. Chitosan oligomers and copper sulfate induce grapevine defense reactions and resistance to gray mold and downy mildew. *Phytopathology* **96**, 1188–1194.
- Bai Z, Harvey LM, McNeil B.** 2003. Oxidative stress in submerged cultures of fungi. *Critical Reviews in Biotechnology* **23**, 267–302.
- Benedetti M, Locci F, Gramegna G, Sestili F, Savatin DV.** 2019. Green production and biotechnological applications of cell wall lytic enzymes. *Applied Sciences* **9**, 5012.
- Benedetti M, Verrascina I, Pontiggia D, Locci F, Mattei B, De Lorenzo G, Cervone F.** 2018. Four Arabidopsis berberine bridge enzyme-like proteins are specific oxidases that inactivate the elicitor-active oligogalacturonides. *The Plant Journal* **94**, 260–273.
- Bhat NN, Padder BA, Barthelson RA, Andrabi KI.** 2019. Compendium of *Colletotrichum graminicola* responsive infection-induced transcriptomic shifts in the maize. *Plant Gene* **17**, 100166.
- Bian C, Duan Y, Xiu Q, Wang J, Tao X, Zhou M.** 2021. Mechanism of validamycin A inhibiting DON biosynthesis and synergizing with DMI fungicides against *Fusarium graminearum*. *Molecular Plant Pathology* **22**, 769–785.
- Bigini V, Camerlengo F, Botticella E, Sestili F, Savatin DV.** 2021. Biotechnological resources to increase disease-resistance by improving plant immunity: a sustainable approach to save cereal crop production. *Plants* **10**, 1146.
- Boedi S, Berger H, Sieber C, Münsterkötter M, Maloku I, Warth B, Strauss J.** 2016. Comparison of *Fusarium graminearum* transcriptomes

on living or dead wheat differentiates substrate-responsive and defense-responsive genes. *Frontiers in Microbiology* **7**, 1113.

**Botticella E, Savatin DV, Sestili F.** 2021. The triple jags of dietary fibers in cereals: how biotechnology is longing for high fiber grains. *Frontiers in Plant Science* **12**, 745579.

**Brown NA, Urban M, Van de Meene AM, Hammond-Kosack KE.** 2010. The infection biology of *Fusarium graminearum*: defining the pathways of spikelet to spikelet colonisation in wheat ears. *Fungal Biology* **114**, 555–571.

**Chanda B, Xia YE, Mandal MK, Yu K, Sekine KT, Gao QM, Kachroo P.** 2011. Glycerol-3-phosphate is a critical mobile inducer of systemic immunity in plants. *Nature Genetics* **43**, 421–427.

**Chang S, Puryear J, Cairney J.** 1993. A simple and efficient method for isolating RNA from pine trees. *Plant Molecular Biology Reporter* **11**, 113–116.

**Chen L, Wang H, Yang J, Yang X, Zhang M, Zhao Z, Wang J.** 2021. Bioinformatics and transcriptome analysis of CFEM proteins in *Fusarium graminearum*. *Journal of Fungi* **7**, 871.

**Chen Q, Tian Z, Jiang R, Zheng X, Xie C, Liu J.** 2018. *StPOTHR1*, a NDR1/HIN1-like gene in *Solanum tuberosum*, enhances resistance against *Phytophthora infestans*. *Biochemical and Biophysical Research Communications* **496**, 1155–1161.

**Cona A, Rea G, Angelini R, Federico R, Tavladoraki P.** 2006. Functions of amine oxidases in plant development and defence. *Trends in Plant Science* **11**, 80–88.

**Conesa A, Götz S, García-Gómez JM, Terol J, Talón M, Robles M.** 2005. Blast2GO: a universal tool for annotation, visualization and analysis in functional genomics research. *Bioinformatics* **21**, 3674–3676.

**Cosgrove D.** 2000. Loosening of plant cell walls by expansins. *Nature* **407**, 321–326.

**Cuomo CA, Güldener U, Xu JR, Trail F, Turgeon BG, Di Pietro A, Kistler HC.** 2007. The *Fusarium graminearum* genome reveals a link between localized polymorphism and pathogen specialization. *Science* **317**, 1400–1402.

**Davidsson P, Broberg M, Kariola T, Sipari N, Pirhonen M, Palva ET.** 2017. Short oligogalacturonides induce pathogen resistance-associated gene expression in *Arabidopsis thaliana*. *BMC Plant Biology* **17**, 19.

**Davis KR, Darvill AG, Albersheim P, Dell A.** 1986. Host-pathogen interactions: XXIX. Oligogalacturonides released from sodium polypectate by endopolygalacturonic acid lyase are elicitors of phytoalexins in soybean. *Plant Physiology* **80**, 568–577.

**De Lorenzo G, Cervone F.** 2022. Plant immunity by damage-associated molecular patterns (DAMPs). *Essays in Biochemistry* **66**, 459–469.

**Denoux C, Galletti R, Mammarella N, Gopalan S, Werck D, De Lorenzo G, Dewdney J.** 2008. Activation of defense response pathways by OGs and Flg22 elicitors in *Arabidopsis* seedlings. *Molecular Plant* **1**, 423–445.

**Desaki Y, Otomo I, Kobayashi D, Jikumaru Y, Kamiya Y, Venkatesh B, Shibuya N.** 2012. Positive crosstalk of MAMP signaling pathways in rice cells. *PLoS One* **7**, e51953.

**Deshaies M, Lamari N, Ng CK, Ward P, Doohan FM.** 2022. The impact of chitosan on the early metabolomic response of wheat to infection by *Fusarium graminearum*. *BMC Plant Biology* **22**, 73.

**Ding L, Xu H, Yi H, Yang L, Kong Z, Zhang L, Ma Z.** 2011. Resistance to hemi-biotrophic *F. graminearum* infection is associated with coordinated and ordered expression of diverse defense signaling pathways. *PLoS One* **6**, e19008.

**Erayman M, Turktas M, Akdogan G, Gurkok T, Inal B, Ishakoglu E, Unver T.** 2015. Transcriptome analysis of wheat inoculated with *Fusarium graminearum*. *Frontiers in Plant Science* **6**, 867.

**Ferrari S, Galletti R, Denoux C, De Lorenzo G, Ausubel FM, Dewdney J.** 2007. Resistance to *Botrytis cinerea* induced in *Arabidopsis* by elicitors is independent of salicylic acid, ethylene, or jasmonate signaling but requires PHYTOALEXIN DEFICIENT3. *Plant Physiology* **144**, 367–379.

**Ferrari S, Savatin DV, Sicilia F, Gramegna G, Cervone F, Lorenzo GD.** 2013. Oligogalacturonides: plant damage-associated molecular patterns and regulators of growth and development. *Frontiers in Plant Science* **4**, 49.

**Francesconi S, Steiner B, Buerstmayr H, Lemmens M, Sulyok M, Balestra GM.** 2020. Chitosan hydrochloride decreases *Fusarium graminearum* growth and virulence and boosts growth, development and systemic acquired resistance in two durum wheat genotypes. *Molecules* **25**, 4752.

**Fraudentali I, Pedalino C, D'Incà R, Tavladoraki P, Angelini R, Cona A.** 2023. Distinct role of AtCuAOβ- and RBOHD-driven H<sub>2</sub>O<sub>2</sub> production in wound-induced local and systemic leaf-to-leaf and root-to-leaf stomatal closure. *Frontiers in Plant Science* **14**, 1154431.

**Galletti R, Denoux C, Gambetta S, Dewdney J, Ausubel FM, De Lorenzo G, Ferrari S.** 2008. The AtrbohD-mediated oxidative burst elicited by oligogalacturonides in *Arabidopsis* is dispensable for the activation of defense responses effective against *Botrytis cinerea*. *Plant Physiology* **148**, 1695–1706.

**Gamir J, Minchev Z, Berrio E, García JM, De Lorenzo G, Pozo MJ.** 2021. Roots drive oligogalacturonide-induced systemic immunity in tomato. *Plant, Cell & Environment* **44**, 275–289.

**Ge SX, Jung D, Yao R.** 2020. ShinyGO: a graphical gene-set enrichment tool for animals and plants. *Bioinformatics* **36**, 2628–2629.

**Gravino M, Locci F, Tundo S, Cervone F, Savatin DV, De Lorenzo G.** 2017. Immune responses induced by oligogalacturonides are differentially affected by AvrPto and loss of BAK1/BKK1 and PEP1/PEP2. *Molecular Plant Pathology* **18**, 582–595.

**Häggblom P, Nordkvist E.** 2015. Deoxynivalenol, zearalenone, and *Fusarium graminearum* contamination of cereal straw; field distribution; and sampling of big bales. *Mycotoxin Research* **31**, 101–107.

**Hahn MG, Darvill AG, Albersheim P.** 1981. Host-pathogen interactions: XIX. The endogenous elicitor, a fragment of a plant cell wall polysaccharide that elicits phytoalexin accumulation in soybeans. *Plant Physiology* **68**, 1161–1169.

**Henrissat B.** 1991. A classification of glycosyl hydrolases based on amino acid sequence similarities. *Biochemical Journal* **280**, 309–316.

**Huang H, Yang X, Zheng M, Chen Z, Yang Z, Wu P, Zhao H.** 2023. An ancestral role for 3-KETOACYL-COA SYNTHASE3 as a negative regulator of plant cuticular wax synthesis. *The Plant Cell* **35**, 2251–2270.

**Iriti M, Varoni EM.** 2017. Moving to the field: plant innate immunity in crop protection. *International Journal of Molecular Sciences* **18**, 640.

**Janda M, Ruelland E.** 2015. Magical mystery tour: salicylic acid signalling. *Environmental and Experimental Botany* **114**, 117–128.

**Jansen C, Von Wettstein D, Schäfer W, Kogel KH, Felk A, Maier FJ.** 2005. Infection patterns in barley and wheat spikes inoculated with wild-type and trichodiene synthase gene disrupted *Fusarium graminearum*. *Proceedings of the National Academy of Sciences, USA* **102**, 16892–16897.

**Jia LJ, Wang WQ, Tang WH.** 2017. Wheat coleoptile inoculation by *Fusarium graminearum* for large-scale phenotypic analysis. *Bio-Protocol* **7**, e2439.

**Jiang C, Zhang C, Wu C, Sun P, Hou R, Liu H, Wang C, Xu JR.** 2016. *TRI6* and *TRI10* play different roles in the regulation of deoxynivalenol (DON) production by cAMP signalling in *Fusarium graminearum*. *Environmental Microbiology* **18**, 3689–3701.

**Jung JY, Kim JH, Baek M, Cho C, Cho J, Kim J, Kim KH.** 2022. Adapting to the projected epidemics of *Fusarium* head blight of wheat in Korea under climate change scenarios. *Frontiers in Plant Science* **13**, 1040752.

**Kazan K, Gardiner DM.** 2018. *Fusarium* crown rot caused by *Fusarium pseudograminearum* in cereal crops: recent progress and future prospects. *Molecular Plant Pathology* **19**, 1547–1562.

**Kubicek CP, Starr TL, Glass NL.** 2014. Plant cell wall-degrading enzymes and their secretion in plant-pathogenic fungi. *Annual Review of Phytopathology* **52**, 427–451.

**Lee T, Lee SH, Shin JY, Kim HK, Yun SH, Kim HY, Ryu JG.** 2014. Comparison of trichothecene biosynthetic gene expression between *Fusarium graminearum* and *Fusarium asiaticum*. *The Plant Pathology Journal* **30**, 33.

**Lionetti V, Fabri E, De Caroli M, Hansen AR, Willats WG, Piro G, Bellincampi D.** 2017. Three pectin methylesterase inhibitors protect cell

- wall integrity for *Arabidopsis* immunity to *Botrytis*. *Plant Physiology* **173**, 1844–1863.
- Liu RQ, Li JC, Wang YS, Zhang FL, Li DD, Ma FX, Chen XL.** 2021. Amino-oligosaccharide promote the growth of wheat, increased antioxidant enzymes activity. *Biology Bulletin* **48**, 459–467.
- Livak KJ, Schmittgen TD.** 2001. Analysis of relative gene expression data using real-time quantitative PCR and the method. *Methods* **25**, 402–408.
- Locci F, Benedetti M, Pontiggia D, Citterico M, Caprari C, Mattei B, De Lorenzo G.** 2019. An *Arabidopsis* berberine bridge enzyme-like protein specifically oxidizes cellulose oligomers and plays a role in immunity. *The Plant Journal* **98**, 540–554.
- Love MI, Huber W, Anders S.** 2014. Moderated estimation of fold change and dispersion for RNA-seq data with DESeq2. *Genome Biology* **15**, 550.
- Luan J, Wei X, Li Z, Tang W, Yang F, Yu Z, Li X.** 2022. Inhibition of chitosan with different molecular weights on barley-borne *Fusarium graminearum* during barley malting process for improving malt quality. *Foods* **11**, 3058.
- Luginbuehl LH, Oldroyd GE.** 2017. Understanding the arbuscule at the heart of endomycorrhizal symbioses in plants. *Current Biology* **27**, R952–R963.
- Maccaferri M, Harris NS, Twardziok SO, Pasam RK, Gundlach H, Spannagl M, Cattivelli L.** 2019. Durum wheat genome highlights past domestication signatures and future improvement targets. *Nature Genetics* **51**, 885–895.
- Magan N, Aldred D.** 2007. Post-harvest control strategies: minimizing mycotoxins in the food chain. *International Journal of Food Microbiology* **119**, 131–139.
- Makandar R, Nalam VJ, Lee H, Trick HN, Dong Y, Shah J.** 2012. Salicylic acid regulates basal resistance to *Fusarium* head blight in wheat. *Molecular Plant-Microbe Interactions* **25**, 431–439.
- Maldonado A, Youssef R, McDonald M, Brewer E, Beard H, Matthews B.** 2014. Overexpression of four *Arabidopsis thaliana* NHL genes in soybean (*Glycine max*) roots and their effect on resistance to the soybean cyst nematode (*Heterodera glycines*). *Physiological and Molecular Plant Pathology* **86**, 1–10.
- Mary Wanjiru W, Zhensheng K, Buchenauer H.** 2002. Importance of cell wall degrading enzymes produced by *Fusarium graminearum* during infection of wheat heads. *European Journal of Plant Pathology* **108**, 803–810.
- Miedaner T.** 1997. Breeding wheat and rye for resistance to *Fusarium* diseases. *Plant Breeding* **116**, 201–220.
- Miedaner T, Sieber AN, Desaint H, Buerstmayr H, Longin CFH, Würschum T.** 2017. The potential of genomic-assisted breeding to improve *Fusarium* head blight resistance in winter durum wheat. *Plant Breeding* **136**, 610–619.
- Miranda JH, Williams RW, Kerven G.** 2007. Galacturonic acid-induced changes in strawberry plant development in vitro. *In Vitro Cellular & Developmental Biology – Plant* **43**, 639–643.
- Montesano M, Kõiv V, Mäe A, Palva ET.** 2001. Novel receptor-like protein kinases induced by *Erwinia carotovora* and short oligogalacturonides in potato. *Molecular Plant Pathology* **2**, 339–346.
- Moscatiello R, Mariani P, Sanders D, Maathuis FJ.** 2006. Transcriptional analysis of calcium-dependent and calcium-independent signalling pathways induced by oligogalacturonides. *Journal of Experimental Botany* **57**, 2847–2865.
- Neubauer M, Serrano I, Rodibaugh N, Bhandari DD, Bautor J, Parker JE, Innes RW.** 2020. *Arabidopsis* EDR1 protein kinase regulates the association of EDS1 and PAD4 to inhibit cell death. *Molecular Plant-Microbe Interactions* **33**, 693–703.
- Norman C, Vidal S, Palva ET.** 1999. Oligogalacturonide-mediated induction of a gene involved in jasmonic acid synthesis in response to the cell-wall-degrading enzymes of the plant pathogen *Erwinia carotovora*. *Molecular Plant-Microbe Interactions* **12**, 640–644.
- Nothnagel EA, McNeil M, Albersheim P, Dell A.** 1983. Host-pathogen interactions: XXII. A galacturonic acid oligosaccharide from plant cell walls elicits phytoalexins. *Plant Physiology* **71**, 916–926.
- Ochoa-Meza LC, Quintana-Obregón EA, Vargas-Arispuro I, Falcón-Rodríguez AB, Aispuro-Hernández E, Virgen-Ortiz JJ, Martínez-Téllez M.** 2021. Oligosaccharins as elicitors of defense responses in wheat. *Polymers* **13**, 3105.
- Osorio S, Castillejo C, Quesada MA, Medina-Escobar N, Brownsey GJ, Suau R, Valpuesta V.** 2008. Partial demethylation of oligogalacturonides by pectin methyl esterase 1 is required for eliciting defence responses in wild strawberry (*Fragaria vesca*). *The Plant Journal* **54**, 43–55.
- Patro R, Duggal G, Love MI, Irizarry RA, Kingsford C.** 2017. Salmon provides fast and bias-aware quantification of transcript expression. *Nature Methods* **14**, 417–419.
- Pfaffl MW.** 2001. A new mathematical model for relative quantification in real-time RT-PCR. *Nucleic Acids Research* **29**, e45.
- Pontiggia D, Benedetti M, Costantini S, De Lorenzo G, Cervone F.** 2020. Dampening the DAMPs: how plants maintain the homeostasis of cell wall molecular patterns and avoid hyper-immunity. *Frontiers in Plant Science* **11**, 613259.
- Pontiggia D, Ciarcianelli J, Salvi G, Cervone F, De Lorenzo G, Mattei B.** 2015. Sensitive detection and measurement of oligogalacturonides in *Arabidopsis*. *Frontiers in Plant Science* **6**, 258.
- Randoux B, Renard-Merlier D, Mulard G, Rossard S, Duyme F, Sanssené J, Reignault P.** 2010. Distinct defenses induced in wheat against powdery mildew by acetylated and nonacetylated oligogalacturonides. *Phytopathology* **100**, 1352–1363.
- Rao S, Zhou Z, Miao P, Bi G, Hu M, Wu Y, Zhou JM.** 2018. Roles of receptor-like cytoplasmic kinase VII members in pattern-triggered immune signaling. *Plant Physiology* **177**, 1679–1690.
- Rasul S, Dubreuil-Maurizi C, Lamotte O, Koen E, Poinssot B, Alcaraz G, Jeandroz S.** 2012. Nitric oxide production mediates oligogalacturonide-triggered immunity and resistance to *Botrytis cinerea* in *Arabidopsis thaliana*. *Plant, Cell & Environment* **35**, 1483–1499.
- Savary S, Willcoquet L, Pethybridge SJ, Esker P, McRoberts N, Nelson A.** 2019. The global burden of pathogens and pests on major food crops. *Nature Ecology & Evolution* **3**, 430–439.
- Savatini DV, Gramegna G, Modesti V, Cervone F.** 2014. Wounding in the plant tissue: the defense of a dangerous passage. *Frontiers in Plant Science* **5**, 470.
- Simpson SD, Ashford DA, Harvey DJ, Bowles DJ.** 1998. Short chain oligogalacturonides induce ethylene production and expression of the gene encoding aminocyclopropane 1-carboxylic acid oxidase in tomato plants. *Glycobiology* **8**, 579–583.
- Soneson C, Love MI, Robinson MD.** 2015. Differential analyses for RNA-seq: transcript-level estimates improve gene-level inferences. *F1000Research* **4**, 1521.
- Sorrentino M, De Diego N, Ugena L, Spíchal L, Lucini L, Miras-Moreno B, Zhang L, Roupheal Y, Colla G, Panzarová K.** 2021. Seed priming with protein hydrolysates improves *Arabidopsis* growth and stress tolerance to abiotic stresses. *Frontiers in Plant Science* **12**, 626301.
- Souza CA, Li S, Lin AZ, Boutrot F, Grossmann G, Zipfel C, Somerville SC.** 2017. Cellulose-derived oligomers act as damage-associated molecular patterns and trigger defense-like responses. *Plant Physiology* **173**, 2383–2398.
- Steiner B, Buerstmayr M, Michel S, Schweiger W, Lemmens M, Buerstmayr H.** 2017. Breeding strategies and advances in line selection for *Fusarium* head blight resistance in wheat. *Tropical Plant Pathology* **42**, 165–174.
- Steiner B, Michel S, Maccaferri M, Lemmens M, Tuberosa R, Buerstmayr H.** 2019. Exploring and exploiting the genetic variation of *Fusarium* head blight resistance for genomic-assisted breeding in the elite durum wheat gene pool. *Theoretical and Applied Genetics* **132**, 969–988.
- Trail F.** 2009. For blighted waves of grain: *Fusarium graminearum* in the postgenomic era. *Plant Physiology* **149**, 103–110.
- Tripathi A, Aggarwal R, Yadav A.** 2013. Differential expression analysis of defense-related genes responsive to *Tilletia indica* infection in wheat. *Turkish Journal of Biology* **37**, 606–613.

- Urban M, Daniels S, Mott E, Hammond-Kosack K.** 2002. Arabidopsis is susceptible to the cereal ear blight fungal pathogens *Fusarium graminearum* and *Fusarium culmorum*. *The Plant Journal* **32**, 961–973.
- van Berkel WJH, Kamerbeek NM, Fraaije M.** 2006. Flavoprotein monooxygenases, a diverse class of oxidative biocatalysts. *Journal of Biotechnology* **124**, 670–689.
- Vanholme R, Cesarino I, Rataj K, Xiao Y, Sundin L, Goeminne G, Boerjan W.** 2013. Caffeoyl shikimate esterase (CSE) is an enzyme in the lignin biosynthetic pathway in *Arabidopsis*. *Science* **341**, 1103–1106.
- Voulgaris I, O'Donnell A, Harvey LM, McNeil B.** 2012. Inactivating alternative NADH dehydrogenases: enhancing fungal bioprocesses by improving growth and biomass yield? *Scientific Reports* **2**, 322.
- Wan J, He M, Hou Q, Zou L, Yang Y, Wei Y, Chen X.** 2021. Cell wall associated immunity in plants. *Stress Biology* **1**, 3.
- Wu G, Liu S, Zhao Y, Wang W, Kong Z, Tang D.** 2015. ENHANCED DISEASE RESISTANCE4 associates with CLATHRIN HEAVY CHAIN2 and modulates plant immunity by regulating relocation of EDR1 in *Arabidopsis*. *The Plant Cell* **27**, 857–873.
- Yang FEN, Jensen JD, Svensson B, Jørgensen HJ, Collinge DB, Finnie C.** 2012. Secretomics identifies *Fusarium graminearum* proteins involved in the interaction with barley and wheat. *Molecular Plant Pathology* **13**, 445–453.
- Yu Y, Yu Y, Cui N, Ma L, Tao R, Ma Z, Meng X, Fan H.** 2022. Lignin biosynthesis regulated by CsCSE1 is required for *Cucumis sativus* defence to *Podosphaera xanthii*. *Plant Physiology and Biochemistry* **186**, 88–98.
- Zhang SB, Zhang WJ, Zhai HC, Lv YY, Cai JP, Jia F, Hu YS.** 2019. Expression of a wheat  $\beta$ -1,3-glucanase in *Pichia pastoris* and its inhibitory effect on fungi commonly associated with wheat kernel. *Protein Expression and Purification* **154**, 134–139.
- Zhang XW, Jia LJ, Zhang Y, Jiang G, Li X, Zhang D, Tang WH.** 2012. *In planta* stage-specific fungal gene profiling elucidates the molecular strategies of *Fusarium graminearum* growing inside wheat coleoptiles. *The Plant Cell* **24**, 5159–5176.